

Absorption, Metabolism, and Excretion of Taselisib (GDC-0032), a Potent β -Sparing PI3K Inhibitor in Rats, Dogs, and Humans^[S]

Shuguang Ma,^{1,2} Sungjoon Cho,¹ Srikumar Sahasranaman,³ Weiping Zhao, Jodie Pang, Xiao Ding, Brian Dean, Bin Wang,⁴ Jerry Y. Hsu,⁵ Joseph Ware,⁶ and Laurent Salphati

Department of Drug Metabolism and Pharmacokinetics (S.M., S.C., W.Z., J.P., X.D., B.D., L.S.) and Department of Clinical Pharmacology (S.S., J.Y.H., J.W.), Genentech, Inc., South San Francisco, California; and XenoBiotic Laboratories (B.W.), Inc., Plainsboro, New Jersey

Received August 29, 2022; accepted December 5, 2022

ABSTRACT

Taselisib (also known as GDC-0032) is a potent and selective phosphoinositide 3-kinase (PI3K) inhibitor that displays greater selectivity for mutant PI3K α than wild-type PI3K α . To better understand the absorption, distribution, metabolism, and excretion properties of taselisib, mass balance studies were conducted following single oral doses of [¹⁴C]taselisib in rats, dogs, and humans. Absolute bioavailability (ABA) of taselisib in humans was determined by oral administration of taselisib at the therapeutic dose followed by intravenous dosing of [¹⁴C]taselisib as a microtracer. The ABA in humans was 57.4%. Absorption of taselisib was rapid in rats and dogs and moderately slow in humans. The recovery of radioactivity in excreta was high (>96%) in the three species where feces was the major route of excretion. Taselisib was the major circulating component in the three species with no metabolite accounting for >10% of the total drug-derived material. The fraction absorbed of taselisib was 35.9% in rats and 71.4% in dogs. In rats, absorbed drug underwent moderate to extensive metabolism and biliary excretion of taselisib was minor. In

dog, biliary excretion and metabolism were major clearance pathways. In humans, 84.2% of the dose was recovered as the parent drug in excreta indicating that metabolism played a minor role in the drug's clearance. Major metabolism pathways were oxidation and amide hydrolysis in the three species while methylation was another prominent metabolism pathway in dogs. The site of methylation was identified on the triazole moiety. In vitro experiments characterized that the N-methylation was dog-specific and likely mediated by a thiol methyltransferase.

SIGNIFICANCE STATEMENT

This study provides a comprehensive description of the absorption, distribution, and metabolism and pharmacokinetic properties of taselisib in preclinical species and humans. This study demonstrated the importance of oral bioavailability results for understanding taselisib's clearance pathways. The study also describes the identification and characterization of a unique dog-specific N-methylation metabolite of taselisib and the enzyme mediating N-methylation in vitro.

Introduction

The phosphoinositide 3-kinase (PI3K) pathway is crucial for the growth, proliferation, and survival of healthy and tumor cells. It is a key pathway that is activated by upstream receptor tyrosine kinases that are known to stimulate cancer cell proliferation, such as human epidermal

growth factor receptor 2, epidermal growth factor receptor, and insulin-like growth factor 1 receptor. Activating mutations, as well as amplification, in the p110 α subunit of PI3K have been identified in many tumor types (Shayesteh et al., 1999; Bachman et al., 2004; Massion et al., 2004; Samuels et al., 2004; Wu et al., 2005). These activating mutations have been shown to promote the growth and invasion in cancer cells that can be abrogated by PI3K inhibitors. The pathway can also be constitutively activated by the loss of the tumor suppressor phosphatase and tensin homolog, a phosphatase that counteracts the kinase activity of PI3K, in many tumor types (Li et al., 1997; Steck et al., 1997). Further downstream, PI3K-pathway activity leads to the phosphorylation and activation of serine/threonine kinase Akt and mammalian target of rapamycin. One of the most mutated oncogenes in hormone-receptor-positive metastatic breast cancer is PIK3CA, the gene encoding for the catalytic subunit of PI3K, which is amplified in 37% and mutated in 9% of squamous lung cancers. As a result, small molecule inhibitors that target the PI3Ks have been actively pursued by pharmaceutical companies as potential treatments for various types of cancers (Shuttleworth et al., 2011).

This work received no external funding.

The authors were employees of Genentech, Inc. or F. Hoffmann-La Roche Ltd when this work was completed.

¹These authors contributed equally.

²Current affiliation: Pharmacokinetics and Drug Metabolism, Amgen, Inc., South San Francisco, California.

³Current affiliation: Clinical Pharmacology, BeiGene, San Mateo, California.

⁴Current affiliation: Ingredient Research, The Coca-Cola Company, Atlanta, Georgia.

⁵Current affiliation: Clinical Development, ArriVent Biopharma, Burlingame, California.

⁶Current affiliation: Clinical Pharmacology, Seagen, South San Francisco, California.
dx.doi.org/10.1124/dmd.122.001096.

[S] This article has supplemental material available at dmd.aspetjournals.org.

ABBREVIATIONS: ABA, absolute bioavailability; ACN, acetonitrile; AMS, accelerator mass spectrometry; AUC, area under the curve; BDC, bile-duct cannulated; CL, clearance; DLC, dog liver cytosol; DLM, dog liver microsome; F_a, fraction absorbed; F_e, fraction excreted; F_g, fraction escaping gut metabolism; F_h, fraction escaping hepatic metabolism; H/D, hydrogen/deuterium; HMBC, heteronuclear multiple bond correlation; HPLC, high-performance liquid chromatography; HSQC, heteronuclear single quantum coherence; LSC, liquid scintillation counters; MetID, metabolite identification; MS, mass spectrometry; NNMT, nicotinamide N-methyltransferase; PI3K, phosphoinositide 3-kinase; PIC, powder-in-capsule; PK, pharmacokinetics; SAM, S-adenosyl-L-methionine; SPE, solid-phase extraction; TMT, thiol methyltransferase; TMPT, thiopurine methyltransferase; TRA, total radioactivity.

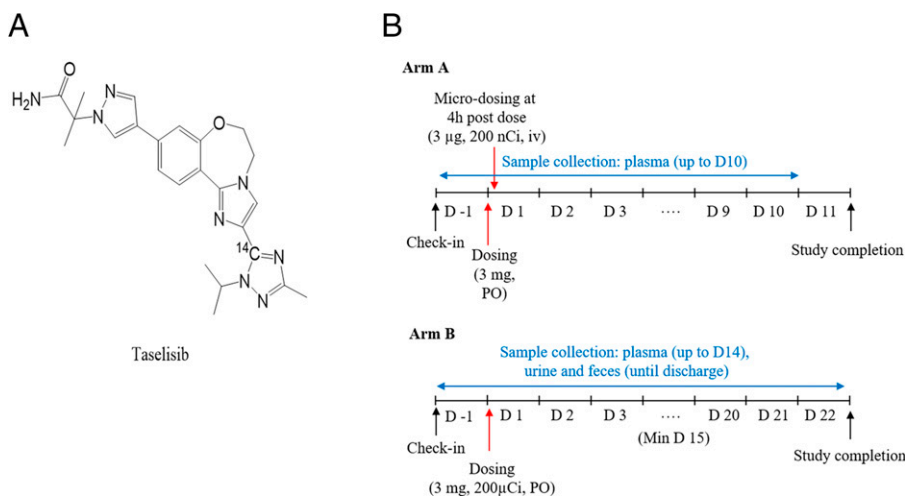


Fig. 1. (A) Structure of taselisib and position of radiolabeling. (B) Study schemes of clinical studies (Arm A and Arm B). D, day; min, minimum.

Taselisib, 2-{3-[2-(1-isopropyl-3-methyl-1*H*-1,2,4-triazol-5-yl)-5,6-dihydrobenzo[*f*]imidazo[1,2-*d*][1,4]oxazepin-9-yl]-1*H*-pyrazol-1-yl]-2-methylpropanamide (also known as GDC-0032) (Fig. 1A) is a potent inhibitor of PI3K that displays greater selectivity for mutant PI3K α isoforms than wild-type PI3K α in vitro (Ndubaku et al., 2013). It has demonstrated activity in nonclinical models of PI3K-mutant tumor cells in vitro and in vivo and has been proven to be potent in nonclinical xenograft models of PI3K-mutant breast tumors. In preclinical studies, taselisib demonstrated promising pharmacokinetic properties, with low plasma clearance (CL) in mice, rats, and monkeys and moderate CL in dogs relative to hepatic blood flow in these species (Ndubaku et al., 2013).

To better understand the absorption, metabolism, and excretion of taselisib in animals and humans, single oral dose studies using ^{14}C -labeled drug were conducted in rats, dogs (preclinical species used for toxicological studies), and humans. Absolute bioavailability was assessed using a microtracer approach in which a ^{14}C -labeled intravenous microdose was concomitantly administered at the T_{max} of an unlabeled therapeutic oral dose. Collectively, these data provided a comprehensive description of the absorption, metabolism, and excretion and pharmacokinetic properties of taselisib in preclinical species and humans.

Materials and Methods

Chemicals and Reagents

^{14}C Taselisib (Fig. 1A) was synthesized by Selcia (Essex, UK) with a specific activity of 55 mCi/mmol. It had a radiochemical purity 99.8% determined by high performance liquid chromatography (HPLC) coupled with in-line radio-detector. Unlabeled taselisib (chemical purity 98.4%) was synthesized at

Genentech, Inc. (South San Francisco, CA). The internal standard for the quantitative LC-MS/MS assays of parent drug was the $^{13}\text{C}_6$ analog of taselisib.

Acetonitrile (ACN) and ultrapure HPLC water were purchased from EMD Chemicals (Gibbstown, NJ). Deuterium oxide (>99% D) was obtained from Thermo Fisher Scientific (Bridgewater, NJ). Ammonium acetate solution (5.0 M) was purchased from Rockland (Gilbertsville, PA). Pico-Fluor 40 carbon-14 cocktail for liquid scintillation counting was from PerkinElmer (Waltham, MA). All other reagents or materials used in these studies were purchased from Sigma-Aldrich (St. Louis, MO) unless otherwise stated. Hepatocytes (human, mouse, rat, dog, and monkey) were purchased from BioreclamationIVT (Westbury, NY). Dog liver microsomes (DLM) and dog liver cytosol (DLC) were purchased from Xenotech (Kansas City, KS). Recombinant dog nicotinamide N-methyltransferase (NNMT) was purchased from SignalChem (Richmond, BC, Canada).

Mass Balance Studies of ^{14}C Taselisib in Rats and Dogs

Rat and dog studies were performed at Covance (Madison, WI). Sprague-Dawley rats were purchased from Hilltop Laboratory Animals (Scottsdale, PA). Beagle dogs were purchased from Covance Research Products (Kalamazoo, MI). Bile-duct cannulated (BDC) rats were provided from Hilltop Laboratory Animals and BDC dogs were prepared by Covance. Animals were fasted overnight before dosing of taselisib and for 4 hours post-dose. BDC animals received bile salts replacement via infusion through the duodenal cannula. The oral formulation for animal studies was 0.5% methylcellulose and 0.2% Tween 80 in water (MCT).

Rats. Four groups of Sprague-Dawley rats were administered a single oral dose at a target dose of 1 mg/kg (100 $\mu\text{Ci/kg}$) of ^{14}C taselisib. Group 1 ($n = 3$ per sex) was used to evaluate excretion mass balance and metabolite profiles in urine and feces collected at pre-dose, 0 to 8, and 8 to 24 hours post-dose and at 24-hour intervals up to 192 hours post-dose. Group 2 included BDC animals ($n = 3$ per sex) for absorption and biliary excretion determination. Bile and urine were collected from Group 2 animals at pre-dose, 0 to 8, and 8 to 24 hours post-

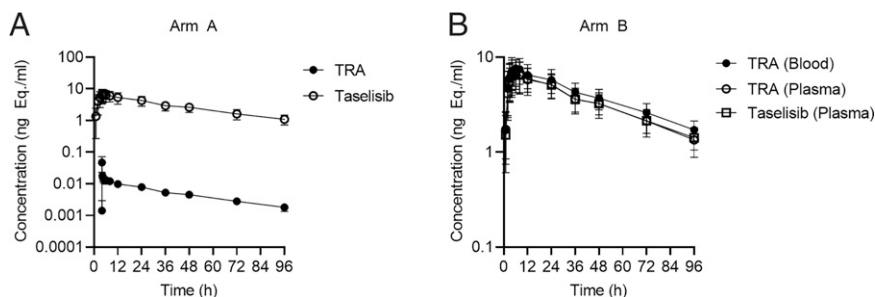


Fig. 2. (A) Plasma taselisib and ^{14}C taselisib concentrations after oral administration of taselisib (3 mg) followed by intravenous administration of ^{14}C taselisib (3 μg , 200 nCi) at 4 hours after oral administration of taselisib in humans (Arm A). (B) Blood and plasma total radioactivity and taselisib concentrations after oral administration of ^{14}C taselisib (3 mg, 200 μCi) in humans (Arm B). TRA and taselisib concentrations in blood and plasma at 336 hours in Arm B were below the limit of quantification. Data are expressed as mean \pm SD.

TABLE 1
Pharmacokinetic parameters in plasma for taselisib and [¹⁴C]tasiselisib in humans after oral administration of taselisib (3 mg) followed by intravenous administration of [¹⁴C]tasiselisib (3 μg, 200 nCi) 4 hours later (Arm A)

	Dose	C _{max} (ng eq/g) ^a	T _{max} (h)	t _{1/2} (h)	AUC ₀₋₄ (ng eq* ^a h/g) ^b	AUC _{0-∞} (ng eq* ^a h/g) ^b	CL/F(L/h) ^c	Vz/F(L) ^{c,e}	AUC _{0-∞} /Dose (ng* ^a h/ml/mg)	F
Oral(tasiselisib)	3 mg	6.96 (3.01)	5.28 (1.23)	40.9 (6.69)	334(116)	342(116)	9.81(3.76)	567 (187)	114(38.6)	0.574 (0.128)
Intravenous ([¹⁴ C]tasiselisib)	3 μg (200 nCi)	47.3 (24.4)	0.05 (0.005)	39.1 (6.17)	574(131)	589(131)	5.28(0.996)	294 (54.1)	196(43.7) ^d	NA

AUC₀₋₄, area under the concentration-time curve from hour 0 to the last measurable concentration; AUC_{0-∞}, area under the concentration-time curve from hour 0 extrapolated to infinity; NA, not applicable.
Data are expressed as mean (SD).
^aUnits for [¹⁴C]tasiselisib are pg equivalents/ml.
^bUnits for [¹⁴C]tasiselisib are pg equivalents*hr/ml.
^cVz: volume of distribution during terminal phase.
^dUnits for [¹⁴C]tasiselisib are pg equivalents*hr/ml/μg.
^eCL and Vz for [¹⁴C]tasiselisib.

dose and at 24-hour intervals up to 168 hours post-dose. Group 3 (*n* = 3 per sex) was designated for pharmacokinetic analysis. From these animals, blood (approximately 0.25 ml) was collected from the jugular vein at pre-dose and at 0.083, 0.25, 1, 3, 6, 12, 24, 48, 72, and 120 hours post-dose and plasma was prepared. Group 4 (*n* = 8 per sex) animals were for profiling of circulating metabolites. One animal per sex was sacrificed via cardiac puncture and as much blood as possible was collected at pre-dose and 0.5, 1, 3, 6, 12, and 48 hours post-dose to provide sufficient plasma for analysis.

Dogs. Male (*n* = 2) and female (*n* = 2) beagle dogs (Group 1) and BDC male beagle dogs (*n* = 2) (Group 2) were administered a single oral dose of [¹⁴C]tasiselisib at a target dose of 2 mg/kg (20 μCi/kg). Urine and feces were collected from animals in Groups 1 (bile duct-intact) and 2 (BDC) at pre-dose, 0 – 8, and 8 – 24 hours post-dose and at 24-hour intervals up to 240 hours post-dose. Bile was collected from male BDC dogs in Group 2 at pre-dose, 0 to 8, and 8 to 24 hours post-dose, and at 24-hour intervals up to 168 hours post-dose. Blood samples were collected from animals in Group 1 and 2 at pre-dose and at 0.083, 0.25, 0.5, 1, 3, 6, 12, 24, 48, 72, 96, 120, 168, and 240 hours post-dose. Blood samples were centrifuged to obtain plasma.

Human Absolute Bioavailability and Mass Balance Study

The clinical portion of this study was conducted by Covance Inc. (Madison, WI) as an open-label, nonrandomized, single-dose study to determine the absolute bioavailability, mass balance, routes of excretion, and metabolite profiling and identification of taselisib in humans. The study consisted of two arms (Arms A and B), where taselisib was administered as both a single oral and intravenous radiolabeled micro-tracer ([¹⁴C]tasiselisib) dose (Arm A) and as a single radiolabeled ([¹⁴C]tasiselisib) oral dose (Arm B). The study schemes of Arm A and Arm B are presented in Fig. 1B. In both Arm A and B, dosing was preceded by an overnight fast (i.e., at least 8 hours) from food (not including water) and was followed by a fast from

food (not including water) for at least 4 hours post-dose following oral dose administration.

In the morning of Day 1, subjects in Arm A of the study (male, *n* = 8) received a single 3-mg oral dose of taselisib [powder-in-capsule (PIC) formulation] with 240 ml of water followed 4 hours later by a single 3-μg i.v. dose of [¹⁴C]tasiselisib containing approximately 200 nCi as a 2 ml manual intravenous push over 3 minutes. Subjects in Arm A were confined for 11 days from the time of check-in (Day –1) until study completion on Day 11.

For Arm B, in the morning of Day 1, subjects in Arm B of the study (male, *n* = 6) received a single 3-mg oral dose of [¹⁴C]tasiselisib (PIC formulation) containing approximately 200 μCi with 240 ml room temperature water. This radioactive dose was selected to ensure that low levels of metabolites would be detectable and was expected to lead to radiation exposure well below (approximately 1% of) the recommended limits in humans, based on dosimetry calculations. Subjects in Arm B were confined from the time of check-in (Day –1) for a minimum of 15 days and a maximum of 22 days, based on subjects meeting the study discharge criteria. Discharge criteria were (1) blood and plasma radioactivity reaches levels below the limit of quantification in two consecutive samples and (2) ≥90% of the dose is recovered or ≤1% of the administered dose is excreted in urine and feces for two consecutive days.

Human Sample Collection

For Arm A, blood samples for pharmacokinetics (PK) analysis of taselisib were collected pre-dose and at 1, 2, 3, 4 (before start of manual intravenous push), 4 hours and 1 minute (i.e., 1 minute into the manual intravenous push), 4 hours and 3 minutes, 4 hours and 15 minutes, 4.5, 5, 6, 8, 12, 24, 48, 72, 96, 120, 168, and 240 hours post-dose. For Arm B, blood samples for PK analysis and metabolite profiling in plasma were collected pre-dose and at 1, 2, 3, 4, 6, 8, 12, 24, 36, 48, 72, 96, 120, 168, 240, and 336 hours post-dose. Urine was collected pre-dose and at 0 to 12 hours and 12 to 24 hours, and then at 24-hour

TABLE 2
Pharmacokinetic parameters in blood, plasma total radioactivity, and plasma taselisib (only humans) in rats, dogs, and humans after oral administration of [¹⁴C]tasiselisib

	Dose ^c	Matix	Analyte	C _{max} (ng eq/g)	T _{max} (h)	t _{1/2} (h)	AUC ₀₋₄ (ng eq* ^a h/g)	AUC _{0-∞} (ng eq* ^a h/g)
Rat ^a	1	Blood	TRA	985 (225)	0.4 (0.3)	3.2 (0.3)	6673 (839)	6718 (847)
		Plasma	TRA	1857 (409)	0.4 (0.3)	3.2 (0.2)	11833 (1385)	11900 (1389)
Dog ^b	2	Blood	TRA	426 (68)	1.5 (1.0)	2.5 (0.1)	2185 (352)	2293 (388)
		Plasma	TRA	415 (84)	1.4 (1.1)	2.5 (0.02)	2138 (436)	2240 (465)
Human (Arm B)	3	Blood	TRA	7.74 (2.61)	5.5 (1.8)	44 (4.2)	411 (114)	492 (127)
		Plasma	TRA	7.14 (2.39)	5.0 (2.0)	39 (6.2)	352 (117)	410 (130)
		Plasma	Tasiselisib	6.92 (2.51)	5.5 (1.8)	42 (4.5)	404 (114)	414 (115)

AUC₀₋₄, area under the concentration-time curve from hour 0 to the last measurable concentration; AUC_{0-∞}, area under the concentration-time curve from hour 0 extrapolated to infinity.
Data are expressed as mean (SD).
^aData from male (*n* = 3) and female (*n* = 3) rats were combined.
^bData from male (*n* = 2) and female (*n* = 2) dogs were combined.
^cDose units are mg/kg for rats and dogs and mg for humans.

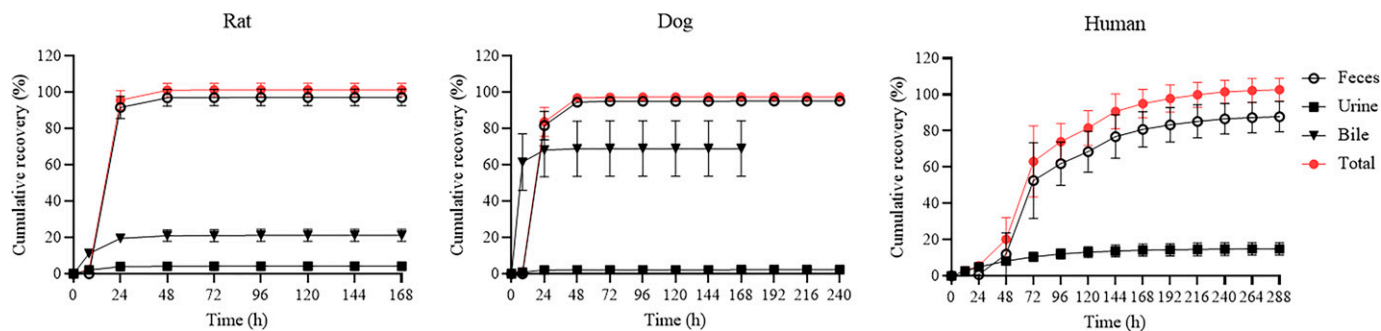


Fig. 3. Cumulative recovery of total radioactivity in urine, feces, and bile after oral administration of [^{14}C]taselisib in rats (1 mg/kg), dogs (2 mg/kg) and humans (3 mg). Data are expressed as mean \pm SD. Bile data from rats and dogs were collected from separate experiments using BDC animals.

intervals until the subject was discharged from the clinical site. Fecal samples were collected predose and at 24-hour intervals until the subject was discharged from the clinical site.

Radioanalysis

The total radioactivity in blood, plasma, urine, and bile from rats and dogs was counted directly by liquid scintillation counters (LSC; PerkinElmer, Waltham, MA). The total radioactivity in human blood and feces from Arm B was combusted in a biologic sample oxidizer and evolved $^{14}\text{CO}_2$ was trapped and analyzed by LSC. The total radioactivity in human plasma and urine from Arm B was analyzed directly by LSC.

Concentrations of total [^{14}C] radioactivity and [^{14}C]taselisib in plasma from Arm A was determined using accelerator mass spectrometry (AMS; (Eckert & Ziegler Vitalea Science, Davis, CA) or HPLC fractionation followed by AMS analysis, respectively. For [^{14}C]taselisib measurement, samples were injected to Zorbax Eclipse XDB-C18 5 μm 2.1 \times 150 mm (Agilent Technologies, CA) after protein precipitation extraction of plasma. The mobile phases were 10 mM ammonium acetate (A) and ACN (B). The gradient started with 20% B and was held for 1 minute, then ramped up to 25% B in 7 minutes. The gradient was then ramped up to 95% B over 4 minutes, held at 95% B for 2 minutes, ramped down to 20% B in 1 minute, and held at 20% B for 5 minutes. The total run time was 20 minutes. The flow rate was 0.75 mL/min.

LC fractions corresponding to [^{14}C]taselisib were collected for AMS analysis. Samples were introduced into the AMS as solid elemental graphite after a two-stage process that involved oxidation to gaseous CO_2 followed by reduction to graphite. The AMS instrument used was the BioMICADAS (PSI/ETH, Zurich, Switzerland).

Extraction of Metabolites from Biologic Samples

Rat. Plasma samples collected from male and female rats in Group 4 at 0.5, 1, 3, 6, and 12 hours post-dose were pooled by gender to generate single pooled samples using the trapezoidal area under the curve (AUC) pooling method (Hop et al., 1998). Plasma samples were protein precipitated by adding ACN followed

by vortex mixing, sonication, and centrifugation. The supernatant was separated, and the procedure was repeated. The combined supernatants were evaporated to dryness and reconstituted with 10 mM ammonium acetate pH 5: ACN (4:1, v:v) for radio-profile analysis.

Urine, feces, and bile samples were pooled from 0 to 48 hours post-dose. Before injection to the LC column, urine and bile samples were centrifuged to remove solid matter. Pooled fecal homogenates were extracted with ACN. The supernatants were evaporated to dryness and reconstituted with 10 mM ammonium acetate pH 5: ACN (4:1, v:v) for radio-profile analysis.

Dog. Plasma samples at pre-dose and 0.083, 0.25, 0.5, 1, 3, 6, and 12 hours post-dose were selected for metabolite profiling. These samples were pooled using the trapezoidal AUC pooling method (Hop et al., 1998). Three volumes of ACN were added to each pooled plasma sample. The samples were mixed by vortex, sonicated, and centrifuged. The supernatants were transferred to a new set of tubes. The extraction procedure was repeated on the post-extraction solids following the same procedures. The supernatants from two extractions were combined, evaporated to near-dryness, and reconstituted with water:ACN (2:1, v/v) for radio-profile analysis.

Urine, feces, and bile samples were pooled from 0 to 48 hours, 0 to 48 hours, and 0 to 24 hours post-dose, respectively. Urine and bile samples from dogs were handled in a same way as to rat urine and bile samples. Pooled fecal homogenates were extracted with ACN, and the supernatants were evaporated to about two-thirds of the original sample weight (v/w) using a SpeedVac and reconstituted with ACN for injection onto an HPLC column.

Human. Plasma samples at pre-dose and 1, 2, 3, 4, 6, 8, 12, 24, 36, 48, 72, and 96 hours post-dose were pooled proportionally to PK AUC separately for each subject (Hop et al., 1998). Three volumes of ACN were added to pooled plasma and the mixture was vortexed, sonicated, and centrifuged. The supernatant was transferred to a new set of tubes. The extraction procedure was repeated on the post-extraction solids following the same procedures. The supernatants from two extractions were combined, evaporated to near-dryness using a SpeedVac concentrator, and reconstituted with H_2O :ACN (2:1, v:v) for radio-profile analysis.

TABLE 3
Percentage of dose recovered after single oral administration of [^{14}C]Taselisib in rats, BDC rats, dogs, BDC dogs, and humans (Arm B)

	Dose ^a	n	Gender	Collection period (h)	Percent dose recovered			
					Urine	Feces	Bile	Total
Rat	1	3	Male	0-192	5.58 (0.550)	94.2 (4.47)	NC	99.8 (4.27)
			Female	0-192	2.97 (0.294)	100 (2.42)	NC	103 (2.82)
Rat (BDC)	1	3	Male	0-168	17.6 (0.146)	NC	19.9 (2.97)	37.5 (3.11)
			Female	0-168	11.7 (2.22)	NC	22.5 (3.69)	34.3 (5.49)
Dog	2	2	Male	0-240	2.18 (NA)	94.1 (NA)	NC	96.3 (NA)
			Female	0-240	2.46 (NA)	96.1 (NA)	NC	98.6 (NA)
Dog (BDC)	2	2	Male	0-240	2.53 (NA)	28.2 (NA)	68.9 (NA)	96.3 (NA)
Human (Arm B)	3	6	Male	0-360	15.0 (3.59)	88.6 (8.23)	NC	104 (6.30)

NA, not applicable; NC, not collected.

Data are expressed as mean (S.D.).

^aDose units are mg/kg for rats and dogs and mg for humans.

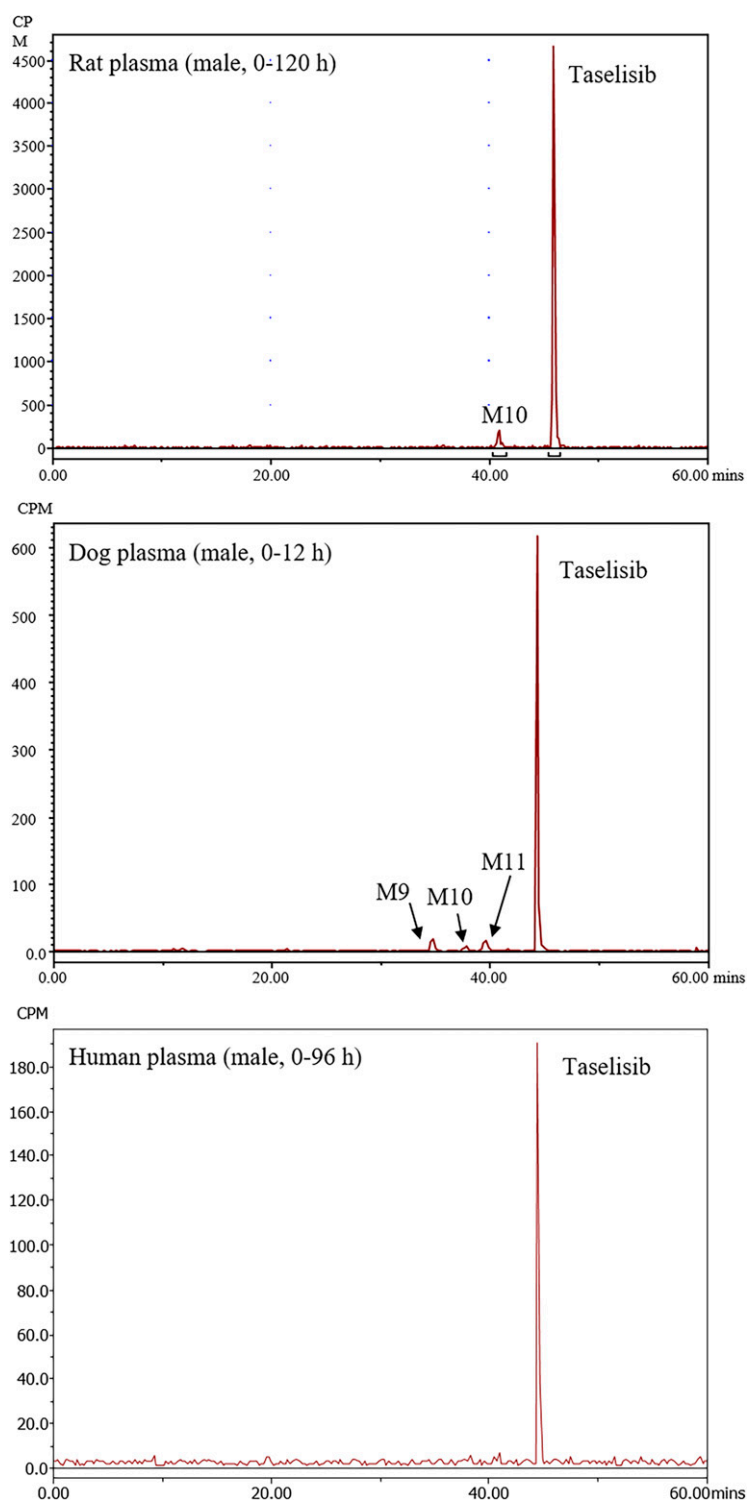


Fig. 4. Representative HPLC radiochromatograms in pooled plasma from rats, dogs, and humans. cpm, count per minute; mins, minutes.

Urine and feces samples were pooled from 0 to 144 hours and 0 to the latest sampling time (i.e., 144, 168, 192, or 216 hours), respectively. Before injection to the LC column, urine samples were centrifuged to remove solid matter. Pooled fecal homogenates were extracted with three volumes of ACN. The extraction was repeated on the post-extraction solids following the same procedures. The supernatants from two extractions were evaporated to about two-thirds of the original sample weight (v/w) using a SpeedVac and reconstituted with ACN for injection onto an HPLC column.

Metabolite Profiling

Liquid chromatography was performed with an Accela ultra-performance liquid chromatography system comprised of a solvent pump with built-in degasser, temperature-controlled autosampler, and photodiode array detector (Thermo Scientific, San Jose, CA). The column used was an Eclipse XDB-C18, 4.6 × 150 mm, 5 μm (Agilent Technologies, Santa Clara, CA) and mobile phases of 10 mM ammonium acetate (pH=5) (mobile phase A) and ACN (mobile phase B) were used. The flow rate was 1 ml/min. The 60-minute-HPLC gradient was

TABLE 4

Distribution^a of radioactive Taselisib and its metabolites in urine, feces, and/or bile from rats, dogs, and humans after oral administration of [¹⁴C]tasisib

Metabolite	Biotransformation	Rat			Dog			Human	
		Urine	Feces	Bile (BDC)	Urine	Feces	Bile (BDC)	Urine	Feces
Tasisib	Parent	0.575	72.1	4.90	0.259	24.8	32.1	12.3	71.9
M1	Oxidation (+32 Da)	0.040	ND	0.995	ND	ND	ND	ND	ND
M2	Glutathione conjugation	ND	ND	0.550	ND	ND	ND	ND	ND
M3	Oxidation (+16 Da)	ND	ND	0.640	ND	ND	ND	ND	ND
M4	Oxidation and glucuronidation	ND	ND	0.760	ND	ND	ND	ND	ND
M5	Di-oxidation (+32 Da)	ND	2.74	0.260	ND	ND	ND	ND	2.65
M6	Oxidative ring opening	ND	ND	0.215	ND	ND	ND	ND	1.44
M7	Oxidation and sulfation	ND	ND	0.175	ND	ND	ND	ND	ND
M8	Oxidation (+16 Da)	0.100	ND	ND	ND	ND	ND	ND	ND
M9	Amide hydrolysis	ND	2.39	7.13	0.516	15.7	9.08	0.825	8.55
M10	Oxidation (+16 Da)	1.760	15.5	3.07	0.258	6.10	1.89	0.697	0.868
M11	Oxidation (+16 Da)	0.230	1.78	0.31	0.622	7.09	4.79	1.23	1.42
M12	Acetylation and ring opening	ND	ND	0.152	ND	ND	ND	ND	ND
M13	Oxidation and glucuronidation	D	D	D	ND	ND	ND	ND	ND
M14	Methylation and oxidation	ND	ND	ND	0.008	0.374	D	ND	ND
M15	Methylation and hydrolysis	ND	ND	ND	0.082	0.346	D	ND	ND
M16	Methylation and oxidation	ND	ND	ND	0.090	11.2	2.95	ND	ND
M17	Methylation	ND	ND	ND	0.222	29.5	18.1	ND	ND
% Dose subtotal		2.68	94.5	19.1	2.06	95.1	68.9	15.0	86.9
% Total excretion		4.27	97.1	21.2	2.32	95.1	68.9	15.0	88.5

D, detected by mass spectrometry; ND, not detected.

^aPercentage of dose identified as tasisib or metabolites.

as follows: mobile phase B was held at 0% for 5 minutes, increased to 5% at 15 minutes, to 20% at 15.1 minutes, to 25% at 40 minutes, to 95% at 50 minutes, held for 5 minutes, then decreased to 0% at 55.1 minutes and held for 5 minutes. The HPLC column effluent was split into radio-detector or fraction collector (0.75 ml/min) and mass spectrometer (0.25 ml/min).

For radio-profiling, the column effluent was directed to a fraction collector and collected on DeepWell LumaPlate-96 microplates (PerkinElmer) on the basis of time. Each fraction was collected for 0.22 minutes. The fractions were evaporated under vacuum and the plates were sealed with transparent TopSeal covers (PerkinElmer). Radioactivity in each well was measured using a TopCount NXT scintillation and luminescence counter (PerkinElmer) for 5 minutes at 20°C. HPLC radio-chromatograms were reconstructed using the LSC import function in Laura evaluation software (LabLogic Systems, Tampa, FL). Radioactive peaks were integrated to calculate the distribution of sample radioactivity and converted to the percentage of the dose by multiplying the distribution by the percentage of administered dose recovered in urine, feces, or bile.

Metabolite Identification

Mass spectrometric (MS) spectra were obtained with an LTQ-Orbitrap high-resolution mass spectrometer operating in a positive ion mode with a heated electrospray ionization source from Thermo Fisher Scientific (San Jose, CA). The electrospray ion source voltage was 4.0 kV and heated capillary temperature was 300°C. The scan-event cycle consisted of a full-scan mass spectrum at resolving power of 30,000, and the corresponding data-dependent scans were acquired at a resolving power of 7,500. Accurate mass measurements were performed using external calibration.

Tasisib Quantitation by LC-MS/MS in Human Plasma

For the determination of Tasisib concentrations in circulation in humans (both Arm A and B), plasma samples were processed with solid phase extraction and the resulting samples were injected to a Pursuit PFP column (5 × 2.0 mm, 3 μm particle size) (Varian, Lake Forest, CA). The LC-MS/MS system consisted of a Shimadzu LC-20 system (Shimadzu Inc., Columbia, MD) coupled with an API 5000 triple quadrupole mass spectrometer (AB Sciex, Foster City, CA). The mobile phases were water containing 0.1% formic acid (A) and ACN with 0.1%

formic acid (B). The gradient started with 30% B and was ramped up to 40% B in 1.5 minutes. The gradient was then ramped down to 30% B over 0.1 minute and was held at 30% B for 0.8 minute. The total run time was 2.4 minutes. The flow rate was 0.5 ml/min. Tasisib and tasisib-d₆ were ionized using an atmospheric pressure chemical ionization source operating in the positive ionization mode. The quantitation of tasisib was performed using MRM transitions with 150 millisecond and 100 millisecond dwell times for tasisib and tasisib-d₆, respectively. Source temperature was 500°C, declustering potential was 110 V, and collision energy was 50 V for tasisib and 40 V for tasisib-d₆. The MRM transitions monitored were m/z 461.5 to m/z 334.2 for tasisib and m/z 467.5 to m/z 420.1 for tasisib-d₆. The method was validated over the calibration curve range 0.400 to 400 ng/ml (Ding et al., 2016).

PK Analysis

PK parameters of total radioactivity and parent drug (in humans only) were calculated by noncompartmental analysis using WinNonlin (version 5.2.1., Pharsight, Mountain View, CA).

Metabolite Isolation of M17 and Structure Characterization by NMR

Dog bile and feces samples across all animals and time intervals were pooled, respectively. Pooled bile sample was processed through solid-phase extraction (SPE) using Oasis HLB 35cc cartridges, while pooled feces sample was extracted with methanol. The extracts were combined, concentrated, fractionated using SPE, then isolated by HPLC. Liquid chromatography was performed with a Waters 2695 Separations Module (Milford, MA) and a Phenomenex Kinetex EVO C₁₈, 5 μm, 150 × 4.6 mm column (Torrance, CA). Mobile phases were 0.05% formic acid in water (mobile phase A) and ACN (mobile phase B). The flow rate was 1 ml/min. The 36 minute-HPLC gradient was as follows: mobile phase B was held at 10% and increased to 40% at 20 minutes, increased to 100% at 21 minutes and held for 5 minutes, then decreased to 10% at 26.01 minutes and held for 10 minutes. The HPLC effluents were collected by time (10 second/fraction) using a Foxy 200 fraction collector. The fractions from 15.5 to 16.2 minutes were combined, dried under a N₂ stream, and further purified using an ion-exchange SPE cartridge (Waters Oasis WCX 3cc) to yield M17 for NMR analysis. Data were

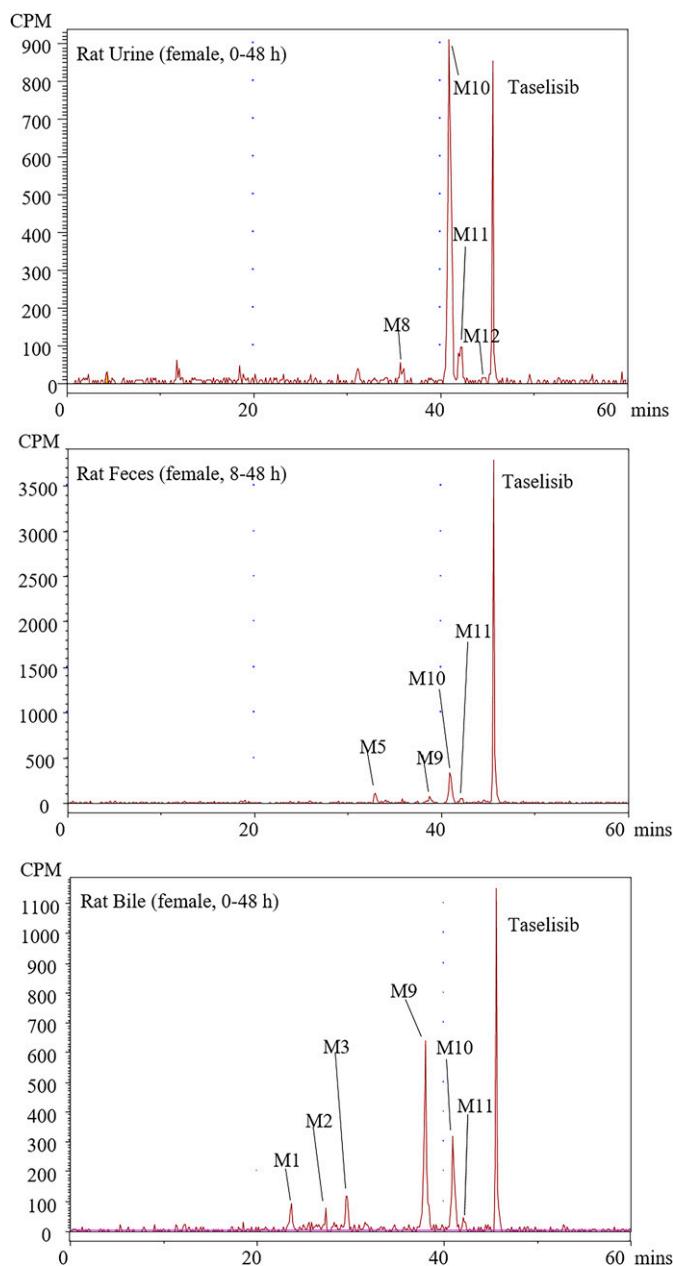


Fig. 5. Representative HPLC radiochromatograms in urine, feces, and bile from rats after oral administration of [^{14}C]Taselisib. cpm, count per minute; mins, minutes.

acquired on a Bruker 500 MHz NMR spectrometer using a 5 mm QNP probe (Billerica, MA).

Hydrogen/Deuterium Exchange LC-MS

For hydrogen/deuterium (H/D) exchange LC-MS experiments to determine the methylation site of M17 in dog samples, deuterium oxide (> 99% D) was used as mobile phase A while all other chromatographic conditions remained the same as described previously and dog samples were analyzed.

In Vitro Experiments

Taselisib (10 μM) was incubated with human, mouse, rat, dog, or monkey hepatocytes (approximately 1.5 million cells/ml) for 3 hours. The reactions were terminated by adding three volume ACN and centrifuged at $2000 \times g$ for

15 minutes. The mixture was evaporated to dryness and reconstituted with 3:1 water to ACN and 10 μL for injection.

To determine the cellular fraction responsible for M17 generation, taselisib (10 μM) was incubated with 3 mg/ml of DLM or DLC in 50 mM phosphate buffer (pH 7.4) containing 5 mM magnesium chloride and 1 mM SAM for 1 hour. The reactions were terminated by adding three volume ACN and centrifuged at $2000 g$ for 15 minutes. The mixture was evaporated to dryness and reconstituted with mixture of water/ACN (3:1) and injected onto LC-MS/MS.

For inhibition assays, taselisib (10 μM) was incubated with dog hepatocytes (cell concentration was approximately 1.5 million cells/ml) in the presence and absence of chemical inhibitors for methyltransferases. The final concentration of inhibitors were 50 μM amodiaquine (histamine N-methyltransferase, histamine N-methyltransferase inhibitor), 5 μM tolcapone (catechol-O-methyltransferase, catechol-O-methyltransferase inhibitor), 50 μM sulfasalazine (thiopurine methyltransferase, TMPT inhibitor), 1 mM 2,3-dichloromethylbenzylamine hydrochloride [thiol methyltransferase (TMT) inhibitor] and 100 μM 1-methyl nicotinamide (NNMT inhibitor) (Maw et al., 2018). The reactions were terminated by adding three volumes of ACN containing 50 nM propranolol and centrifuged at $2000 g$ for 15 minute. The mixture was evaporated to dryness and reconstituted with mixture of water/ACN (3:1) and injected onto LC-MS/MS.

Additional incubations with taselisib (10 μM) and 2 $\mu\text{g/ml}$ of recombinant dog NNMT were conducted in 50 mM phosphate buffer (pH 7.4) containing 5 mM magnesium chloride and 1 mM SAM in the presence and absence of 5-amino-1-methylquinolin-1-ium iodide (20 μM , a NNMT inhibitor). As a positive control, nicotinamide, a known substrate of NNMT was incubated with NNMT. The mixture was preincubated for 5 minutes in water bath at 37°C , followed by the addition of 1 mM SAM to start the reaction. After 1 hour, the reactions were terminated by adding three volumes of ACN with 50 nM propranolol and centrifuged at $2000 g$ for 15 minutes. The mixture was evaporated to dryness and reconstituted with mixture of water/ACN (3:1) and injected onto LC-MS/MS.

Samples from in vitro experiments were analyzed using an LTQ-Orbitrap Velos mass spectrometer (Thermo Scientific) equipped with an Accela ultra performance liquid chromatography. For taselisib and methylation-related metabolites, liquid chromatography for was performed with a Kinetex 2.6 μm , XB-C18 100A 100x2.1 mm column (Phenomenex) and mobile phases of 10 mM ammonium acetate (pH 5) (mobile phase A) and ACN (mobile phase B). The flow rate was 0.4 ml/min. The 23 minute-HPLC gradient was as follows: mobile phase B was held at 2% for 2 minutes, increased to 50% at 15 minute, to 95% at 15.5 minute and held for 2 minute, then decreased to 2% at 18 minute and held for 5 minute.

For nicotinamide and 1-methyl nicotinamide, liquid chromatography was performed with a Synergi 2.5 μm , Polar RP 100A 100 \times 2 mm column (Phenomenex) and mobile phases of 10 mM ammonium acetate (pH 5) (mobile phase A) and ACN (mobile phase B). The flow rate was 0.4 ml/min. The 15 minute-HPLC gradient was as follows: mobile phase B was started at 1% and held for 9 minutes, increased to 95% at 9.1 minute, and held at 95% for 2.4 minute, then decreased to 1% at 11.6 minute and held for 3.4 minute.

Results

Pharmacokinetics and Absolute Bioavailability of Taselisib in Humans

A summary of PK parameters following administration of 3 mg oral taselisib and 3 μg (200 nCi) IV [^{14}C]taselisib in Arm A is presented in Table 1. The concentration-time profiles for taselisib and [^{14}C]taselisib in plasma for Arm A are presented in Fig. 2A. Following oral administration of 3 mg taselisib, the rate of absorption of taselisib was moderate with average T_{max} of 5.28 hours. After reaching C_{max} , taselisib plasma concentrations appeared to decline in a biphasic manner with a mean terminal half-life ($t_{1/2}$) of 40.9 hours. The mean CL/F and V_z/F values for taselisib in plasma were 9.81 L/h and 567 L, respectively. Following IV administration of 3 μg (200 nCi) [^{14}C]taselisib, plasma radioactivity declined in parallel to the taselisib concentrations with a mean terminal ($t_{1/2}$) of 39.1 hours. The mean CL and V_z values for [^{14}C]taselisib in

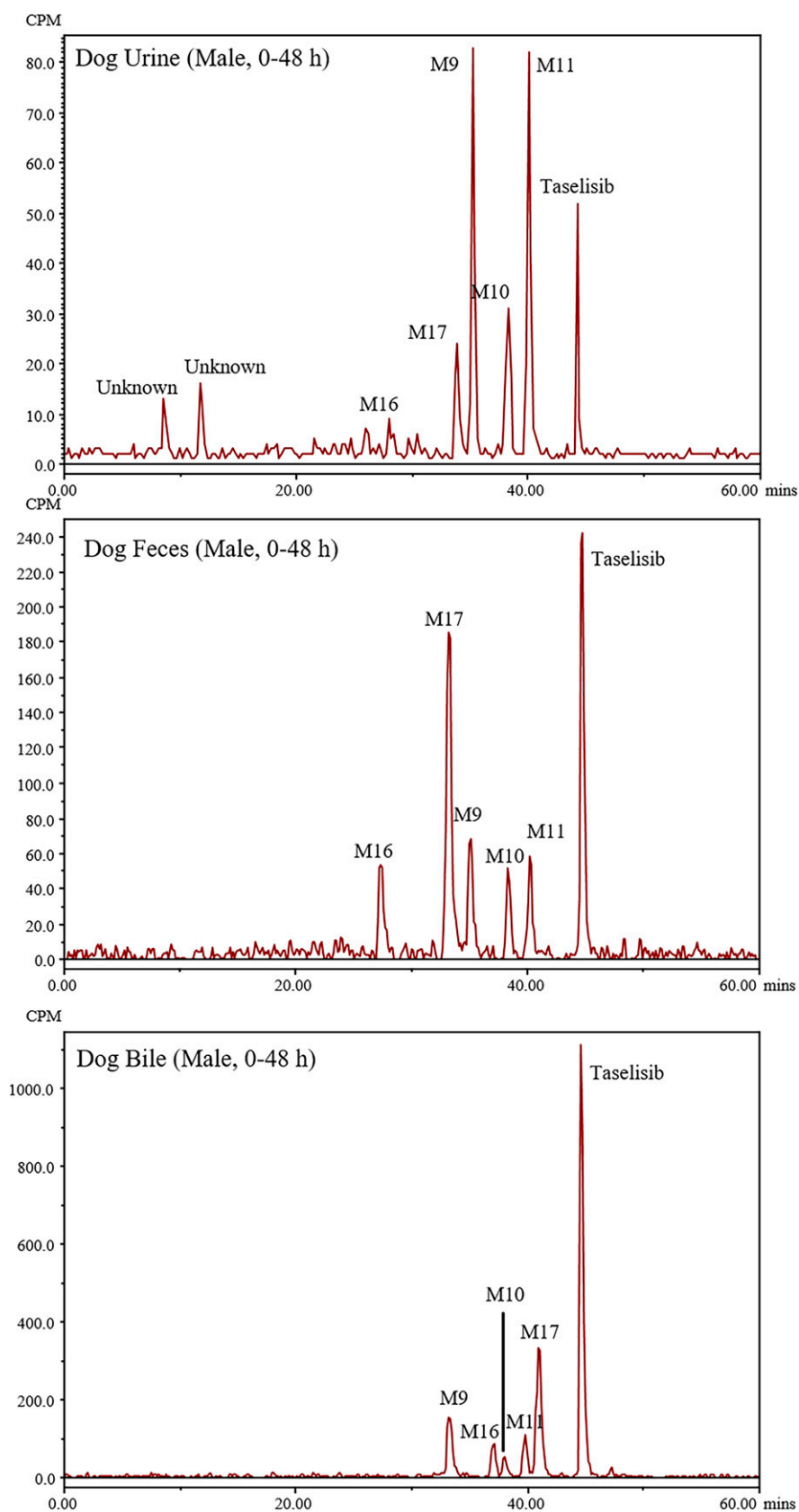


Fig. 6. Representative HPLC radiochromatograms in urine, feces, and bile from dogs after oral administration of $[^{14}\text{C}]$ Taselisib. cpm, count per minute; mins, minutes.

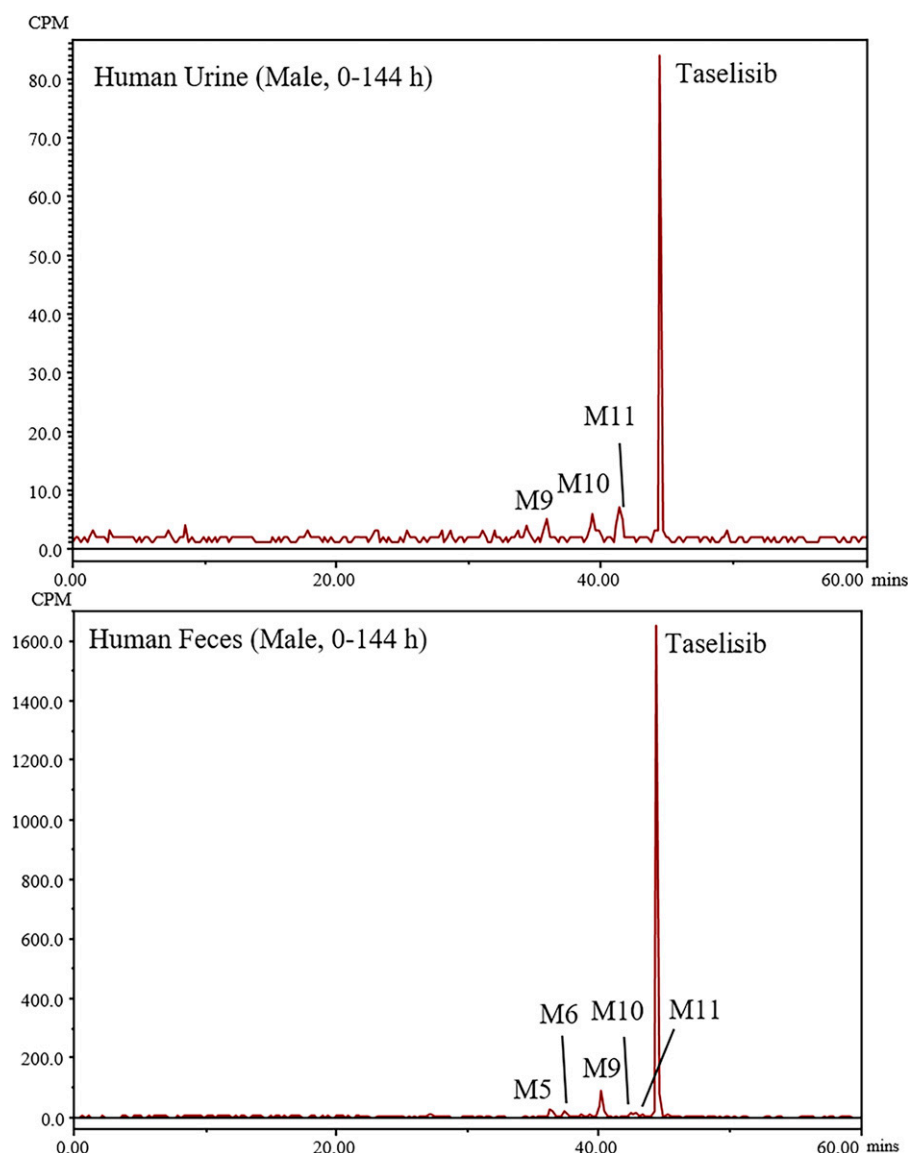


Fig. 7. Representative HPLC radiochromatograms in urine and feces from humans after oral administration of [^{14}C]Taselisib. cpm, count per minute; mins, minutes.

plasma were 5.28 L/h and 294 L, respectively. The mean absolute bio-availability (F) of taselisib following oral administration was 57.4%.

Blood and Plasma Total Radioactivity in Rats, Dogs and Humans

Pharmacokinetic parameters of blood and plasma total radioactivity (TRA) in rats, dogs and humans, and plasma taselisib in humans are summarized in Table 2. The blood and plasma concentration-time profiles of TRA and plasma taselisib concentration-time profile in humans are shown in Fig. 2B. Since concentration and pharmacokinetic data indicated that there were no apparent gender differences in rats and dogs, data from male and female animals were averaged.

In rats, C_{\max} of blood and plasma TRA were 985 and 1857 ng-Eq/g, respectively. T_{\max} was 0.4 hour suggesting the absorption of taselisib was rapid. Both blood and plasma $t_{1/2}$ were 3.2 hour. Mean blood:plasma concentration ratios, where calculable, ranged from 0.495 through 0.744 (data in file) indicating minimal association of drug-derived radioactivity with the cellular component of blood.

In dogs, C_{\max} of blood and plasma TRA were 426 and 415 ng-Eq/g, respectively. T_{\max} was 1.5 hour after dosing suggesting that taselisib was readily absorbed. Both blood and plasma $t_{1/2}$ were 2.5 hour. The

average blood to plasma concentration ratios ranged from 0.936 to 1.14 indicating that the radioactivity was not preferentially distributed to the cellular component of the blood in dogs.

In humans, T_{\max} of TRA and taselisib in plasma were 5 and 5.5 hours respectively, suggesting moderate to slow absorption. After reaching C_{\max} plasma concentrations declined in a biphasic manner, with mean terminal $t_{1/2}$ values of approximately 42, 39, and 44 hours observed for taselisib in plasma, TRA in plasma, and TRA in blood, respectively. The mean blood/plasma ratio for total radioactivity was approximately 1.23 for $\text{AUC}_{0-\infty}$ indicating low association of radioactivity with red blood cells. The longer T_{\max} observed in humans compared with rats and dogs was most likely due to the difference in formulation, with rats and dogs receiving a homogenous MCT suspension, and humans being administered a PIC.

Excretion and Mass Balance

The cumulative recoveries of the administered radioactivity in urine, feces, and bile from rats, dogs and humans are shown in Table 3 and Fig. 3.

Rat. Following a single oral dose of [^{14}C]taselisib, radioactivity was rapidly excreted and the excretion of radioactivity was nearly complete

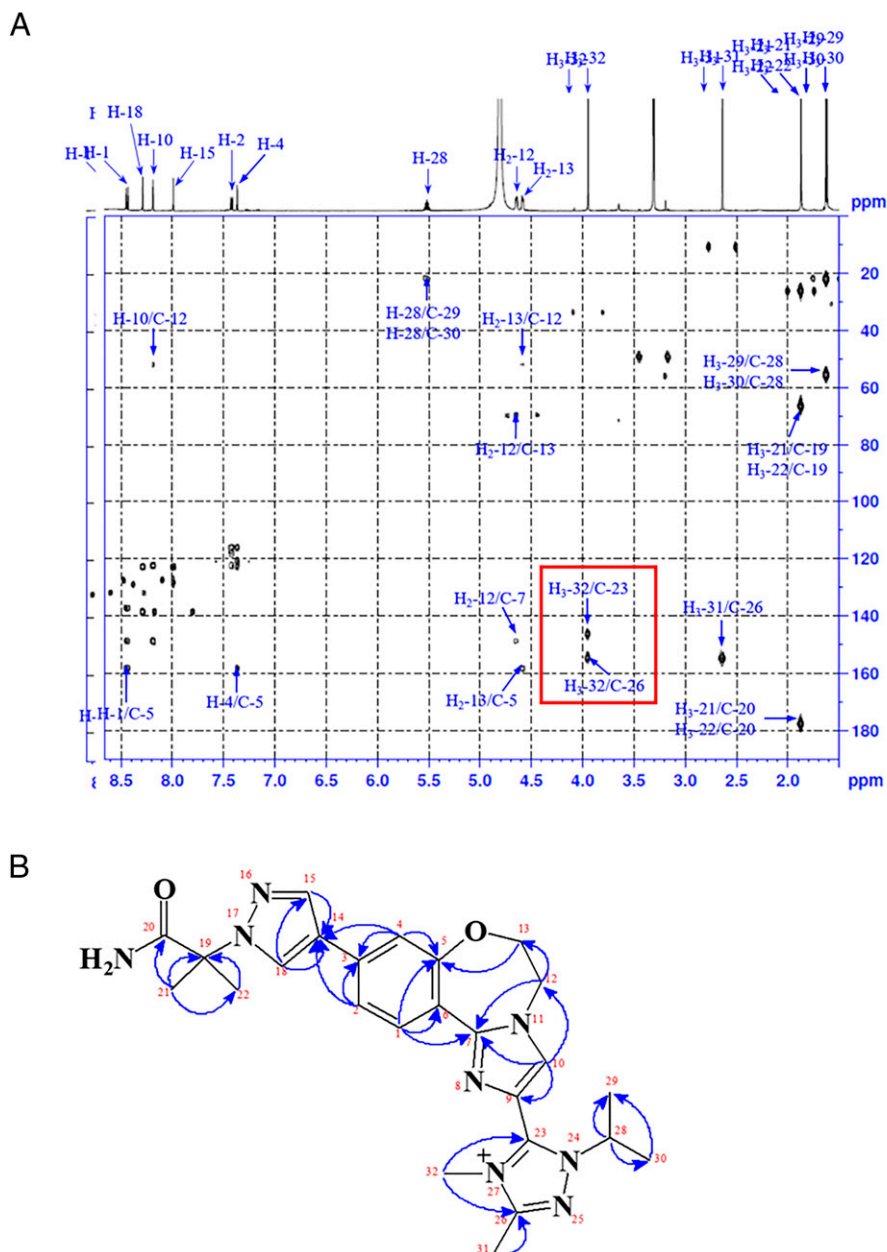


Fig. 8. (A) HMBC spectrum for M17 (500 MHz, CD₃OD) and (B) key HMBC correlations of M17.

by 24 hours post-dose. There was no gender difference in excretion of radioactivity. The predominant route of elimination of [^{14}C]taselisib-derived radioactivity was via feces accounting for 94.2% and 100% of the administered dose through 192 hours post-dose in male and female rats, respectively. Urinary excretion of radioactivity accounted for 5.58% and 2.97% of the dose through 192 hours post-dose in male and female rats, respectively. Biliary excretion of radioactivity through 168 hours post-dose in BDC rats accounted for 19.9% and 22.5% of the dose in male and female rats, respectively. Urinary excretion of radioactivity in BDC rats was 17.6% and 11.8% of the dose in male and female rats, respectively. Biliary and urinary recoveries of the administered dose indicated that absorption of [^{14}C]taselisib was approximately 36%, suggesting low to moderate absorption of taselisib.

Dog. The excretion profiles in bile duct-intact male and female dogs were similar. Radioactivity was eliminated rapidly, with averages of

97% of the administered dose recovered by 48 hours post-dose. The predominant route of elimination was via feces which accounted for 94.1% and 96.1% of the dose in male and female dogs, respectively. Urinary excretion was minimal and accounted for 2.18% and 2.46% of the dose in male and female dogs, respectively. In BDC male dogs, the majority of the radioactivity (68.9% of the administered dose) was recovered in bile, suggesting that biliary excretion played a major role in the elimination of [^{14}C]taselisib. The urinary excretion in BDC dogs accounted for 2.53% of the administered dose. Biliary and urinary recoveries of the administered dose indicated that absorption of [^{14}C]taselisib was approximately 72% of the administered dose, suggesting high absorption of taselisib in dogs.

Humans. Most of the administered radioactivity was recovered in the first 144 hours post-dose (90.6%). The overall mean recovery of radioactivity in urine and feces samples was 104% over the 360-hour

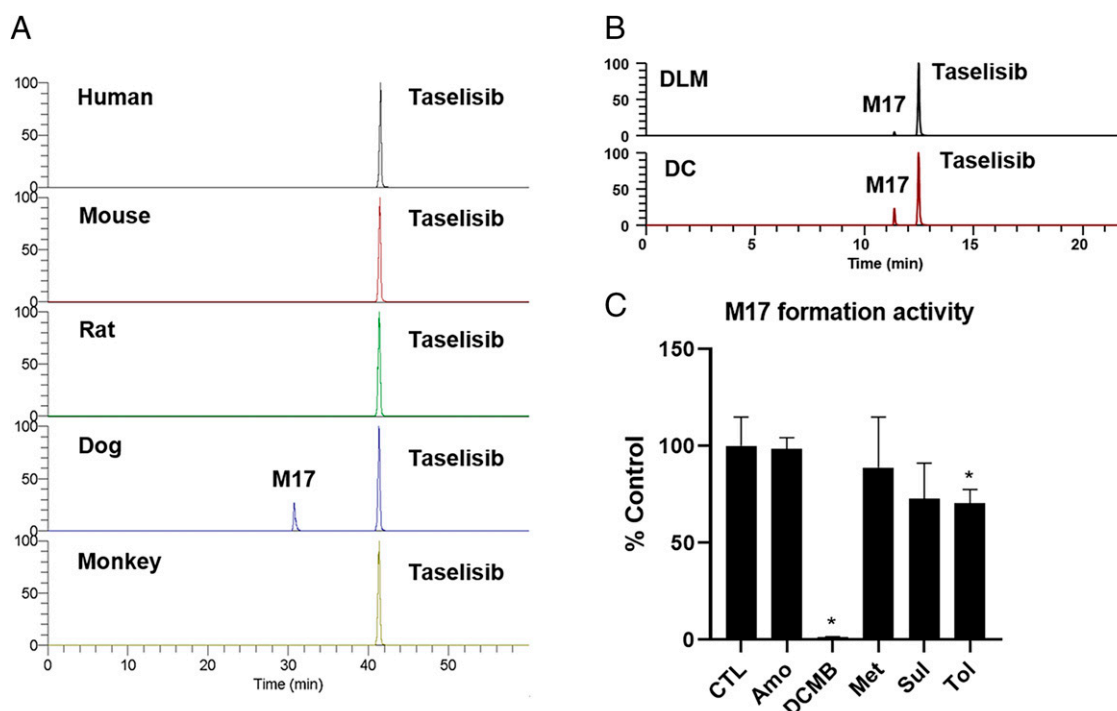


Fig. 9. Characterization of methyltransferases involved in M17 formation in dogs. (A) Tasisib was incubated with human, mouse, rat, dog, and monkey hepatocytes for 3 hours. Extracted ion chromatogram of M17 and tasisib was presented. (B) Tasisib was incubated with dog liver microsome and dog liver cytosol. Extracted ion chromatogram of M17 and tasisib was presented. (C) Tasisib was incubated with dog hepatocytes in the presence of various methyltransferase inhibitors for 3 hours: central limit theorem; DMSO vehicle control. $P < 0.05$ compared with CTL from student t test. Amo, amodiaquine (histamine N-methyltransferase inhibitor); COMT, catechol-O-methyltransferase; DCMB, 2,3-dichloromethylbenzylamine hydrochloride (TMT inhibitor); Met, 1-methyl nicotinamide (NNMT inhibitor); Sul, sulfasalazine (TPMT inhibitor); Tol, tolcapone (COMT inhibitor). * $P < 0.05$ compared with CTL from student t test.

study. A mean of 88.6% of the dose was recovered in feces and 15.0% was recovered in urine through the last collection interval, suggesting that the predominant route of elimination was via feces.

Structural Characterization and Identification of Tasisib Metabolites

The metabolites identified in this study with molecular ions, major fragments and sources where the metabolites were detected are listed in Supplementary Table 1. Seventeen metabolites were identified in rats, dogs or humans and structure elucidations were performed with LC-MS/MS. Structures of M17 was confirmed by H/D exchange LC-MS and NMR.

Circulating Metabolites of Tasisib in Rats, Dogs and Humans

Representative HPLC radiochromatograms of pooled plasma from rats, dogs and humans are shown in Fig. 4.

Rats. No gender-dependent differences in plasma metabolite profiles were observed in rats. Radio-profiles in pooled plasma from rats showed that tasisib accounted for 94.1% of sample radioactivity and M10 (hydroxylation) accounted for 5.03%.

Dog. No gender-dependent differences in plasma metabolite profiles were observed in dogs. Tasisib was the most abundant drug-related material in pooled plasma accounting for 88.6% of the total plasma sample radioactivity. Four minor metabolites were detected, which were M9 (amide hydrolysis), M10 (oxidation), M11 (oxidation) and M17 (methylation), accounting for 3.90%, 1.84%, 4.55% and 1.13% of the total plasma sample radioactivity, respectively. M14 (methylation and oxidation), M15 (hydrolysis and methylation), and M16 (methylation and oxidation) were of minor abundance and were only detected by mass spectrometry.

Human. Tasisib was the only detectable radioactive peak in the pooled 0-96 hour plasma from all six subjects, indicating that tasisib

was the predominant drug-derived material in the circulation. No metabolite was detected in circulation.

Metabolite Profiles of Tasisib in Urine, Feces, and Bile

Urine, feces, and bile collections were pooled to represent > 90% of the total radioactivity in the corresponding excretion routes and profiled to determine the distribution of metabolites (Table 4).

Rat. Representative HPLC radiochromatograms of urine, feces and bile from rats are shown in Fig. 5. Radio-analysis of rat urine showed one prominent metabolite, M10 (1.76% of administered dose), and numerous minor radioactive peaks in addition to [^{14}C]tasisib, all of which accounted for less than 0.575% of administered dose. Radio-analysis of fecal samples showed that tasisib was the major radioactive component and accounted for 72.1% of administered dose. The most abundant metabolite was M10, accounting for 15.5% of administered dose. M5, M9 and M11 were also detected, accounting for 2.74, 2.39 and 1.78%, respectively. In bile samples from BDC rats, M9 was the most abundant metabolite and accounted for 7.13% of administered dose. Biliary excretion of [^{14}C]tasisib was minor and accounted for 4.9% of the administered dose. M10 was also observed in bile accounting 3.07% of the administered dose. Numerous minor metabolites were observed including M1, M2, M3, M4, M5, M6, M7, M11 and M12, all of which accounted for less than 1% of the administered dose. Major metabolism pathways in rats were oxidation (M10) and hydrolysis of amide (M9).

Dog. Representative HPLC radiochromatograms of urine, feces and bile from dogs are shown in Fig. 6. In urine, tasisib represented only 0.259% of the administered dose. Four relatively abundant urinary metabolites (M17, M9, M10, and M11) were characterized, representing 0.222%, 0.516%, 0.258%, and 0.622% of the dose, respectively. Other

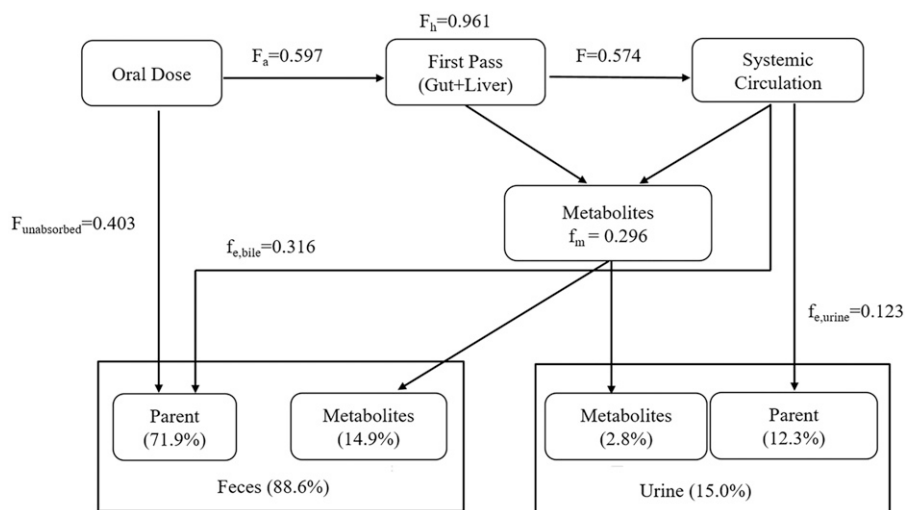


Fig. 10. Proposed disposition of taselisib after oral administration in humans.

minor metabolites included M14, M15, and M16, and accounted for less than 0.1% of the dose.

In fecal samples from bile duct-intact dog, unchanged taselisib represented 24.8% of the administered dose, indicating that taselisib was extensively metabolized in dogs. Methylation metabolite, M17 was the most abundant metabolite in feces and accounted for 29.5% of the dose. Other major fecal metabolites included M9, M10, M11 and M16 representing 15.7%, 6.10%, 7.10% and 11.2%, of the dose, respectively. M14 and M15 were also detected, but were less than 0.5% of the dose. Methylation related metabolites (M14-M17) in feces together accounted for 41.4% of the dose, suggesting methylation was a major metabolism pathway.

In dog bile, taselisib accounted for 32.1% of the administered dose indicating that biliary secretion of unchanged drug was a major clearance pathway in dogs. The major metabolites in bile were M17 and M9, accounting for 18.1% and 9.08% of the dose, respectively. Other minor metabolites included M10, M11 and M16, which represented 1.89%, 4.79% and 2.95% of the administered radioactivity, respectively. Major metabolism pathways in dogs were methylation (M17), oxidation (M10, M11) and hydrolysis of amide (M9).

Human. Representative HPLC radiochromatograms of urine and feces from humans are shown in Fig. 7. In urine, unchanged taselisib was the most abundant drug derived material and accounted for 12.3% of the dose. Three urinary metabolites (M9, M10, and M11) were detected accounting for 0.825%, 0.697% and 1.23% of the dose, respectively.

In fecal samples, unchanged taselisib was the most abundant component and represented 71.9% of the dose. M9 was the major metabolite in feces and accounted for 8.55% of the dose. Other fecal metabolites included M5, M6, M10 and M11, representing 2.65%, 1.44%, 0.868%, and 1.42% of the dose, respectively. Major metabolism pathways in humans were hydrolysis of amide (M9) and oxidation (M5, M6, M11).

Structure Characterization of M17 by H/D Exchange LC-MS and NMR

H/D exchange LC-MS experiments were performed to facilitate the structural characterization of the methylation metabolites of taselisib. The molecular ion of taselisib was observed at m/z 464.2596 following H/D exchange, which was 3 Da higher than that observed with non-deuterated mobile phases (data in file). The 3-Da mass increase for $[M + H]^+$ of taselisib is consistent with the exchange of two hydrogen atoms at the amide and the ionizing proton in $[M + H]^+$ with

deuteriums. The molecular ion of M17 in deuterated solvent was detected at m/z 477.2692, which was 2 Da higher than that detected in non-deuterated mobile phases, corresponding to the exchange of two hydrogen atoms at the amide with deuteriums. This result indicated that M17 does not require an ionizing proton, suggesting that the metabolite most likely contains a quaternary ammonium cation. Therefore, methylation had probably occurred on the nitrogen of triazole, imidazole or pyrazole ring. Similarly, the molecular ions of M14, M15 and M16 were observed at m/z 494.2712, m/z 477.2480, and m/z 494.2712, which were 3 Da, 1 Da, and 3 Da higher than those observed with non-deuterated mobile phases, respectively and suggested that methylation on those metabolites also likely occurred on the nitrogen of triazole, imidazole or pyrazole ring to form quaternary ammonium cations.

M17 was isolated and purified from dog bile and feces samples for definitive structure characterization using NMR. 1D (1H) and 2D [heteronuclear single quantum coherence (HSQC) and heteronuclear multiple bond correlation (HMBC)] NMR techniques were performed to elucidate the structure of M17. Likewise, the NMR data of taselisib were also obtained for comparison purpose. 1H and ^{13}C NMR assignments of taselisib and M17 are summarized in Supplementary Table 2.

M17 has been characterized as an N-methyl metabolite. Proton and carbon chemical shifts of the additional methyl group of M17 (δH 3.95, δC 33.6) (Supplementary Table 2) confirmed the presence of an N-methyl moiety. Key HMBC spectrum and correlations of M17 are depicted in Fig. 8 (HSQC data are in file). HMBC correlations from H3-32 to C-23 and C-26 were observed, indicating the methylation occurred on the N-27 of the triazole moiety.

In Vitro Characterization of Enzymes Involved in Methylation of Taselisib in Dogs

In vitro experiments were conducted to determine the enzymes involved in the methylation of taselisib to M17. Hepatocytes from 5 species (human, mouse, rat, dog and monkey) were incubated with taselisib and only dog hepatocytes generated M17 (Fig. 9A). This was consistent with in vivo data showing that M17 was only observed in dogs, not in rats or humans. Both DLM and DLC were able to generate M17 from taselisib (Fig. 9B), suggesting that multiple methyltransferases located in DLC or DLM were involved in the methylation of taselisib. In dog hepatocytes incubated with various methyltransferase inhibitors, DCMB significantly inhibited the formation of M17 (approximately 98%) while others showed minimal or moderate (< 30%)

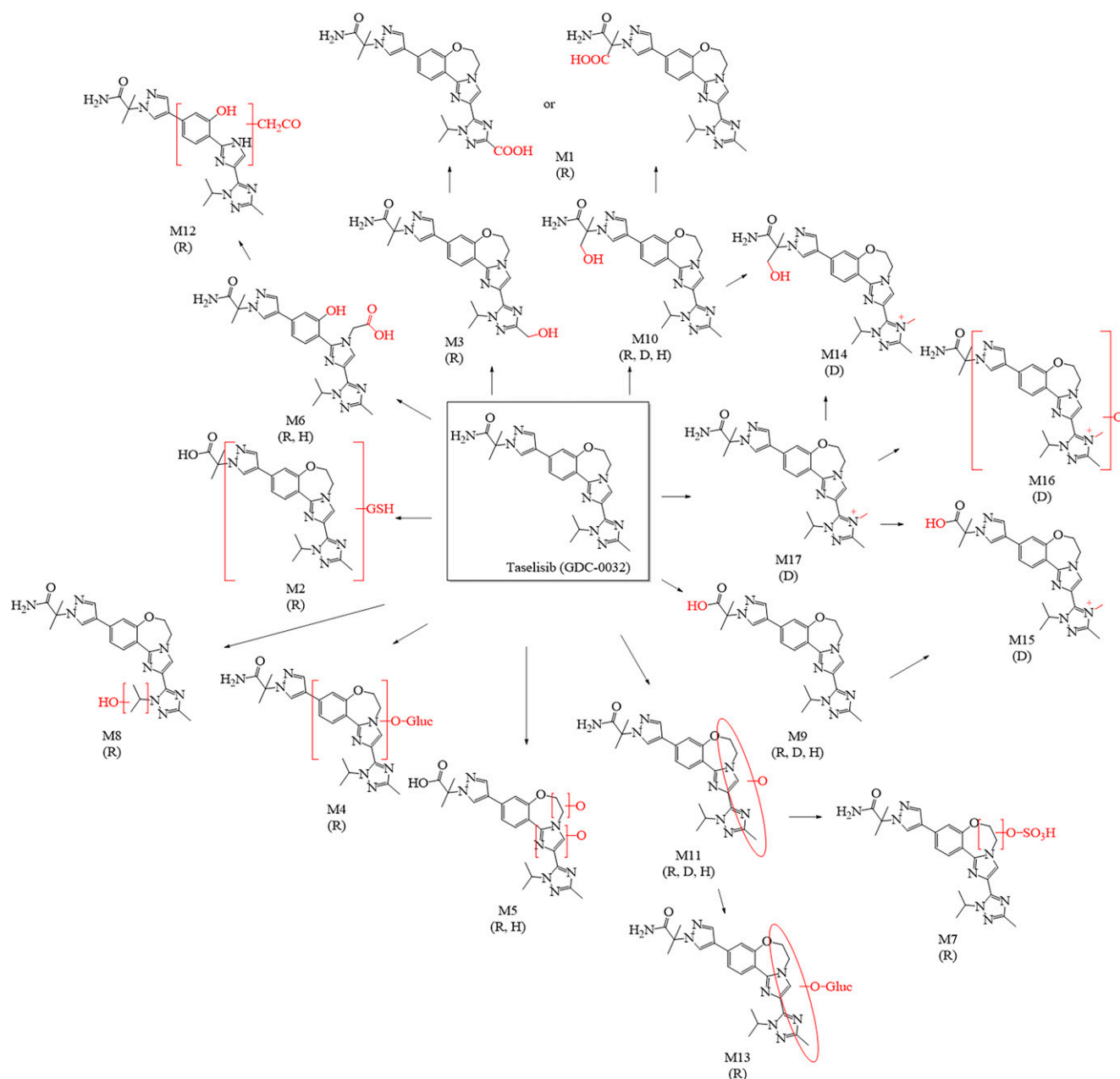


Fig. 11. Proposed major metabolic pathways of taselisib in rats (R), dogs (D), and humans (H).

inhibition activity. Methylation-related metabolites M15 and M16 showed similar trend (Supplementary Figure S1) while M14 was not observed in dog hepatocytes. Recombinant dog NNMT was incubated with taselisib which showed minimal generation of M17 while it significantly methylated nicotinamide (a known substrate of NNMT) (Supplementary Figure S1C) confirming that NNMT was likely not involved in the methylation of taselisib.

Discussion

In the current study, the absorption, metabolism, and excretion of taselisib were characterized after a single oral dose in rats, dogs and humans.

In humans, the ABA of taselisib following a single oral dose of 3 mg taselisib as PIC was determined to be 57.4%. A relative BA study conducted later showed that the exposure obtained with the final tablet

formulation was approximately 1.5-fold greater than that achieved with the PIC formulation (Faber et al., 2016). No further ABA study was performed with the tablet.

The study design with intravenous microtracer had numerous benefits. The number of healthy volunteers could be reduced and no wash-out period was needed in contrast to traditional absolute bioavailability studies. Since i.v. microtracer was given at the T_{max} of orally administered taselisib in which the body was already exposed to the drug at the therapeutic dose, the possibility of non-linear PK of intravenous microtracer was eliminated. This allows for comparison of the oral and IV doses when there are therapeutically relevant concentrations of drug systemically available. Additionally, simultaneous dosing resulted in less variability in the absolute bioavailability estimate, and ensured the systemic clearance was consistent for the IV and oral doses. A stable isotope labeled microtracer with LC-MS/MS analysis would be a good

alternative approach for ABA (Ma and Chowdhury, 2016). However, because the LC-MS/MS method could not achieve the required sensitivity at low pg/ml and the synthesis of another stable-labeled drug for IV microtracer presented technical difficulties, this approach was not used for this study.

Whole blood and plasma total radioactivity data suggested that all three species showed minimal association of drug-derived radioactivity with the cellular component of blood. The $t_{1/2}$ of TRA was comparable in rats and dogs, while that in humans was markedly longer, in agreement with the slower excretion of total radioactivity compared with rats and dogs (Fig. 4). This long $t_{1/2}$ in humans was underpredicted by the non-clinical data and PBPK modeling, mainly due to an overprediction of CL, as previously described (Heffron et al., 2022). Even though humans showed long $t_{1/2}$ of TRA, retention of radioactivity in the body was expected to be minimal based on the good mass balance achieved (almost 100% of the dose excreted in urine and feces) and the marginal contribution of AUC from the β -phase (i.e., terminal phase) to the total AUC (Table 1). Plasma TRA and tasiselisib concentrations in humans were almost identical (Fig. 3C), which is consistent with minimal circulating metabolites detected in plasma (Fig. 5).

The fraction absorbed (Fa) of tasiselisib was moderate in rats (35.9%) and high in dogs (71.4%) based on the sum of % dose excreted in the bile (Table 3) and urine in BDC animals. The fraction absorbed in humans (Fa) following oral dose could not be determined from this study since the parent drug recovered in feces (88.6% of the administered dose) could come from the unabsorbed drug, biliary excretion of the absorbed drug, or both. Instead, we estimated Fa by the following calculations: Results from the ABA study indicated that the average bioavailability (F) of tasiselisib in humans was 0.574. According to mass balance and MetID results, 12.3% of dose in urine was unchanged tasiselisib ($f_{e,urine}=0.123$) and plasma renal CL was calculated to be 1.13 L/h ($[CL_{r,p} = (fe/F)*CL_{iv}]$). Therefore, hepatic plasma clearance ($CL_{h,p}$) was 4.15 L/h ($CL_{iv}-CL_{r,p}$) and hepatic blood clearance ($CL_{h,b}$) was 3.37 L/h ($CL_{h,b} = CL_{h,p}/(C_b/C_p)$). Accordingly, F_h was estimated to be 0.961 ($F_h = 1 - CL_{h,b}/Q_h$) and hence, fraction absorbed (Fa) in humans was estimated to be at least 0.597 ($Fa = F/(F_h * F_g)$) assuming F_g was approximately 1. The estimated Fa was within the ranges of Fa values observed in rats and dogs. Fa of 0.597 suggested that unabsorbed fraction of tasiselisib was 0.403. Therefore approximately 32% of the dose as parent in feces was from biliary excretion ($F_{e,bile}$ = fraction of unchanged parent excreted in feces – fraction of unabsorbed parent = $0.719 - 0.403 = 0.316$). Total metabolites in excreta represented 17.7% of dose. Therefore, f_m (fraction metabolized) was estimated to be 0.296 ($0.177/Fa$). The proposed disposition of tasiselisib after oral administration in humans based on these calculations is summarized in Fig. 10. The estimation of the various fractions available (Fa, F_h) and the insight gained into the clearance pathways ($f_{e,bile}$ and f_m) relied on the determination of the oral bioavailability. This further emphasizes the importance of ABA studies in providing key information for the understanding of the disposition and clearance of orally administered compounds, such as tasiselisib.

In dogs, humans, and to a much lesser extent in rats, biliary elimination of unchanged tasiselisib was observed or estimated. This excretion was most likely mediated by P-glycoprotein and/or BCRP, since this compound is a substrate of both transporters (Pang et al., 2014) and studies in Pgp/BCRP knock-out mice and rats confirmed the prominent roles these transporters play in the biliary elimination of tasiselisib (Salphati, 2018). In addition, in a clinical DDI study, itraconazole co-administration led to 1.5-fold increase in the AUC of tasiselisib (Sahasranaman et al., 2015), which could be explained by inhibition of CYP3A4. However, considering that tasiselisib undergoes very limited metabolism, it is possible also that the higher exposure observed resulted from the inhibition of Pgp and/or BCRP by itraconazole. Taken together,

these data suggest that the elimination of tasiselisib in the bile is mediated by Pgp and/or BCRP in preclinical species and humans.

Proposed metabolic pathways of tasiselisib in rats, dogs and humans are presented in Fig. 11. In rats, absorbed [^{14}C]tasiselisib underwent moderate to extensive metabolism and major metabolic pathways were hydrolysis to produce M9 and hydroxylation to produce M10.

In dogs, approximately 25% of the administered dose was recovered as the parent drug in urine and feces from the bile duct–intact dogs, indicating that tasiselisib was extensively metabolized. The major metabolic pathways included methylation, amide hydrolysis, oxidation, and the combination of oxidation and methylation. Methylation was only observed in dogs. Interestingly, percentage dose of M10 and M11 were higher in feces than that in bile in both rats and dogs suggesting that M10 and M11 could be also generated in the intestine or secreted directly from the systemic circulation into the intestine.

In contrast to rats and dogs, approximately 84.2% of the dose was recovered as the parent drug in humans, indicating that tasiselisib was mainly cleared as unchanged drug in urine and feces. Metabolism played a relatively minor role in the drug's clearance in humans. Major biotransformation pathway were amide hydrolysis and oxidation. The overall turnover of tasiselisib in vitro was very low. The hydrolytic metabolite M9 was barely detected, at the limit of quantitation, in hepatocyte incubations. These conditions did not allow us to study and identify the enzymes involved in the formation of M9.

Mass balance studies suggested that dogs exclusively produced N-methylation metabolites and in vitro hepatocytes experiments also confirmed that N-methylation was dog-specific. Species differences in N-methylation activity of pyridine were reported in vivo (D'Souza et al., 1980; Damani et al., 1982) and dog-specific N-methylation activities were also reported. Leeson et al. reported the N-methylation of oxprenolol in beagle dogs (Leeson et al., 1973) while Walle et al. reported a dog-specific N-methylation of N-demethylated metabolites of propranolol, alprenolol and oxprenolol (Walle et al., 1981). N-methylation and quaternization have been reported in a few nitrogen-containing heterocycles similar to N-methylation of tasiselisib (Damani and Case, 1984). For example, N-methylation of pyridine ring such as N-methylnicotine, N-methylcotinine, ethionamide and N-methylation of the thiazole ring of anticonvulsant drug, chlormethiazole were reported (Damani and Case, 1984). To our knowledge, N-methylation of tasiselisib is the first example of N-methylation on triazole ring, which expands our knowledge about the chemical moieties potentially undergoing N-methylation.

There are a wide range of methyltransferase reported to mediate xenobiotic metabolisms and their cellular locations are cytosol or microsomes (Jancova et al., 2010). In vitro experiment showed that both dog liver cytosol and microsomes could mediate N-methylation of tasiselisib suggesting that multiple methyltransferases were involved in that reaction. Several methyltransferase inhibitors were tested and 2,3-dichloromethylbenzylamine (DCMB) significantly inhibited the methylation of tasiselisib (98%). DCMB is a TMT inhibitor (Maw et al., 2018). TMT is located mainly in microsomes (Kazui et al., 2014), but several studies showed that TMT activity was also detected in cytosol (Glauser et al., 1992; Liu et al., 2015; Maw et al., 2018). Although TMT is widely known to mediate S-methylation of a wide range of compounds (Obach et al., 2012; Kazui et al., 2014; Liu et al., 2015), N-methylation activity of TMT was also reported (Maw et al., 2018). Therefore, TMT might play a role in the methylation of tasiselisib in dogs, though this study cannot rule out that other methyltransferases might also be involved in the methylation of tasiselisib because DCMB might also inhibit other methyltransferases in dogs. The role of another N-methyltransferase, NNMT, on the N-methylation of tasiselisib was investigated using the recombinant dog enzyme. The data suggested that dog NNMT played a minor role, which was consistent with the minimal effect of the NNMT

inhibitor 1-methyl nicotinamide, on tasisib methylation. It is worth noting though, that the specificity of 1-methyl nicotinamide for the dog enzyme is not as established as it is for the human NNMT.

In summary, this study comprehensively characterized the absorption, metabolism, and excretion of tasisib in rats, dogs, and humans. Absolute bioavailability of tasisib was also determined in humans. Overall, mass balance of tasisib was similar in the three species where fecal excretion was the major route of excretion. Tasisib was the major circulating component with minor metabolites in all three species. Major metabolism pathways were oxidation and amide hydrolysis in the three species while methylation was also a major metabolism pathway in dogs. Structures of dog-specific methylation metabolites and enzymes potentially mediating methylation were characterized.

Acknowledgments

The authors wish to thank the patients for enrolling in this study and taking valuable time away from their personal lives to advance science. The authors also wish to thank all principal investigators and their staff for the conduct of the clinical study. Their support is gratefully acknowledged.

Author Contributions

Participated in research design: Ma, Cho, Dean, Salphati.

Conducted experiments: Ma, Cho, Zhao, Ding.

Performed data analysis: Ma, Cho, Sahasranaman, Zhao, Pang, Ding, Dean, Hsu, Ware, Salphati.

Wrote or contributed to the writing of the manuscript: Ma, Cho, Zhao, Dean, Salphati.

References

- Bachman KE, Argani P, Samuels Y, Silliman N, Ptak J, Szabo S, Konishi H, Karakas B, Blair BG, Lin C et al. (2004) The PIK3CA gene is mutated with high frequency in human breast cancers. *Cancer Biol Ther* 3:772–775.
- Damani L and Case D (1984) Metabolism of heterocycles, in *Comprehensive Heterocyclic Chemistry* (Katritzky AR and Rees CW), 1:39–89, Pergamon Press, Oxford.
- Damani LA, Crooks PA, Shaker MS, Caldwell J, D'Souza J, and Smith RL (1982) Species differences in the metabolic C- and N-oxidation, and N-methylation of [14C]pyridine in vivo. *Xenobiotica* 12:527–534.
- Ding X, Faber K, Shi Y, McKnight J, Dorshorst D, Ware JA, and Dean B (2016) Validation and determination of tasisib, a β -sparing phosphoinositide 3-kinase (PI3K) inhibitor, in human plasma by LC-MS/MS. *J Pharm Biomed Anal* 126:117–123.
- D'Souza J, Caldwell J, and Smith RL (1980) Species variations in the N-methylation and quaternization of [14C]pyridine. *Xenobiotica* 10:151–157.
- Faber KP, Borin MT, Cheeti S, Fraczekiewicz G, Nelson E, Ran Y, Dresser MJ, Graham RA, Sahasranaman S, Hsu J et al. (2016) Impact of formulation and food on tasisib (GDC-0032) bioavailability: powder-in-capsule formulation represents unique drug development challenge. *Clin Pharmacol Ther* 99:PI-067.
- Glauser TA, Kerremans AL, and Weinshilboum RM (1992) Human hepatic microsomal thiol methyltransferase. Assay conditions, biochemical properties, and correlation studies. *Drug Metab Dispos* 20:247–255.
- Heffron TP, Salphati L, and Staben ST (2022) Discovery of tasisib (GDC-0032), in: *Contemporary Accounts in Drug Discovery and Development* (Huang X, Aslanian RG, and Tang WH, eds), pp. 145–156, Wiley, Hoboken, NJ.
- Hop CE, Wang Z, Chen Q, and Kwei G (1998) Plasma-pooling methods to increase throughput for in vivo pharmacokinetic screening. *J Pharm Sci* 87:901–903.
- Jancova P, Anzenbacher P, and Anzenbacherova E (2010) Phase II drug metabolizing enzymes. *Biomed Pap Med Fac Univ Palacky Olomouc Czech Repub* 154:103–116.
- Kazui M, Hagiwara K, Izumi T, Ikeda T, and Kurihara A (2014) Hepatic microsomal thiol methyltransferase is involved in stereoselective methylation of pharmacologically active metabolite of prasugrel. *Drug Metab Dispos* 42:1138–1145.
- Leeson GA, Garteiz DA, Knapp WC, and Wright GJ (1973) N-methylation, a newly identified pathway in the dog for the metabolism of oxprenolol, a beta-receptor blocking agent. *Drug Metab Dispos* 1:565–568.
- Li J, Yen C, Liaw D, Podypanina K, Bose S, Wang SI, Puc J, Milaresis C, Rodgers L, McCombie R et al. (1997) PTEN, a putative protein tyrosine phosphatase gene mutated in human brain, breast, and prostate cancer. *Science* 275:1943–1947.
- Liu C, Chen Z, Zhong K, Li L, Zhu W, Chen X, and Zhong D (2015) Human liver cytochrome P450 enzymes and microsomal thiol methyltransferase are involved in the stereoselective formation and methylation of the pharmacologically active metabolite of clopidogrel. *Drug Metab Dispos* 43:1632–1641.
- Ma S and Chowdhury SK (2016) The use of stable isotope-labeled drug as microtracers with conventional LC-MS/MS to support human absolute bioavailability studies: are we there yet? *Bioanalysis* 8:731–733.
- Massion PP, Taflan PM, Shyr Y, Rahman SM, Yildiz P, Shakhthour B, Edgerton ME, Ninan M, Andersen JJ, and Gonzalez AL (2004) Early involvement of the phosphatidylinositol 3-kinase/Akt pathway in lung cancer progression. *Am J Respir Crit Care Med* 170:1088–1094.
- Maw HH, Zeng X, Campbell S, Taub ME, and Teitelbaum AM (2018) N-Methylation of BI 187004 by thiol S-methyltransferase. *Drug Metab Dispos* 46:770–778.
- Ndubaku CO, Heffron TP, Staben ST, Baumgardner M, Blaquiery N, Bradley E, Bull R, Do S, Dotson J, Dudley D et al. (2013) Discovery of 2-[3-[2-(1-isopropyl-3-methyl-1H-1,2,4-triazol-5-yl)-5,6-dihydrobenzo[f]imidazo[1,2-d][1,4]oxazepin-9-yl]-1H-pyrazol-1-yl]-2-methylpropanamide (GDC-0032): a beta-sparing phosphoinositide 3-kinase inhibitor with high unbound exposure and robust in vivo antitumor activity. *J Med Chem* 56:4597–4610.
- Obach RS, Prakash C, and Kamel AM (2012) Reduction and methylation of ziprasidone by glutathione, aldehyde oxidase, and thiol S-methyltransferase in humans: an in vitro study. *Xenobiotica* 42:1049–1057.
- Pang J, Baumgardner M, Cheong J, Edgar K, Heffron TP, Le H, Ndubaku O, Olivero AG, Plise EG, Staben ST et al. (2014) Preclinical evaluation of the β isoform-sparing PI3K inhibitor GDC-0032 and prediction of its human pharmacokinetics. *Drug Metab Rev* 45(Suppl):219.
- Sahasranaman S, Graham RA, Salphati L, Hsu J, Lu X, Gates M, Amin D, Bradford D, Dresser M, and Ware J (2015) Assessment of pharmacokinetic interaction between the PI3K inhibitor tasisib (GDC-0032) and a strong CYP3A4 inducer or inhibitor. *Clin Pharmacol Ther* 97:PII-073.
- Salphati L (2018) Interaction of the PI3kinase inhibitor tasisib with efflux transporters: in vivo and in vitro investigations. *Paper presented at the SMI ADMET Conference, London*.
- Samuels Y, Wang Z, Bardelli A, Silliman N, Ptak J, Szabo S, Yan H, Gazdar A, Powell SM, Riggs GJ et al. (2004) High frequency of mutations of the PIK3CA gene in human cancers. *Science* 304:554.
- Shayesteh L, Lu Y, Kuo WL, Baldocchi R, Godfrey T, Collins C, Pinkel D, Powell B, Mills GB, and Gray JW (1999) PIK3CA is implicated as an oncogene in ovarian cancer. *Nat Genet* 21:99–102.
- Shuttleworth SJ, Silva FA, Cecil AR, Tomassi CD, Hill TJ, Raynaud FI, Clarke PA, and Workman P (2011) Progress in the preclinical discovery and clinical development of class I and dual class I/IV phosphoinositide 3-kinase (PI3K) inhibitors. *Curr Med Chem* 18:2686–2714.
- Steck PA, Pershouse MA, Jasser SA, Yung WK, Lin H, Ligon AH, Langford LA, Baumgard ML, Hattier T, Davis T et al. (1997) Identification of a candidate tumour suppressor gene, MMAC1, at chromosome 10q23.3 that is mutated in multiple advanced cancers. *Nat Genet* 15:356–362.
- Walle UK, Wilson MJ, and Walle T (1981) Propranolol, alprenolol and oxprenolol metabolism in the dog. Identification of N-methylated metabolites. *Biomed Mass Spectrom* 8:78–84.
- Wu G, Xing M, Mambo E, Huang X, Liu J, Guo Z, Chatterjee A, Goldenberg D, Gollin SM, Sukumar S et al. (2005) Somatic mutation and gain of copy number of PIK3CA in human breast cancer. *Breast Cancer Res* 7:R609–R616.

Address correspondence to: Dr. Laurent Salphati, Drug Metabolism and Pharmacokinetics, Genentech, Inc., 1 DNA Way, South San Francisco, CA 94080. E-mail: salphati.laurent@gene.com

Drug Metabolism and Disposition

DMD-AR-2022-001096

Supplementary data

Absorption, Metabolism, and Excretion of Taselisib (GDC-0032), a Potent β -sparing PI3K

Inhibitor, in Rats, Dogs, and Humans

Shuguang Ma^{*},¹, Sungjoon Cho^{*}, Srikumar Sahasranaman², Weiping Zhao, Jodie Pang, Xiao Ding, Brian Dean, Bin Wang³, Jerry Y. Hsu⁴, Joseph Ware⁵, Laurent Salphati

Department of Drug Metabolism and Pharmacokinetics (SM, SC, WZ, JP, XD, BD, LS) and

Department of Clinical Pharmacology (SS, JH, JW), Genentech, Inc., 1 DNA Way, South San Francisco, CA, 94080; XenoBiotic Laboratories (BW), Inc., 107 Morgan Lane, Plainsboro, NJ 08536

^{*} Contributed equally

¹Current affiliation: Pharmacokinetics and Drug Metabolism, Amgen, Inc., South San Francisco, CA

²Current affiliation: Clinical Pharmacology, BeiGene, San Mateo, CA

³Current affiliation: Ingredient Research, The Coca-Cola Company, Atlanta, GA

⁴Current affiliation: Clinical Development, ArriVent Biopharma, Burlingame, CA

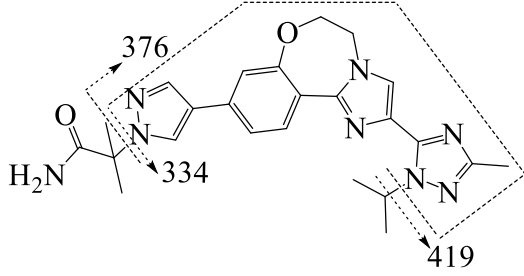
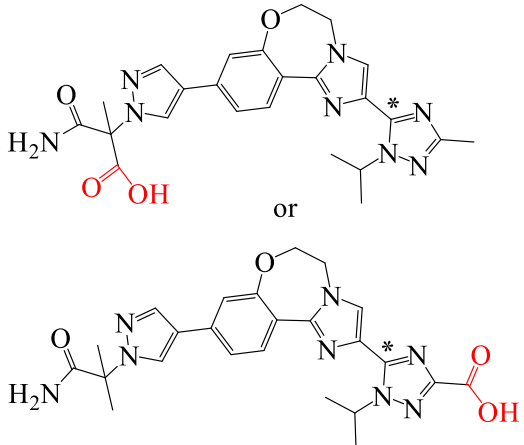
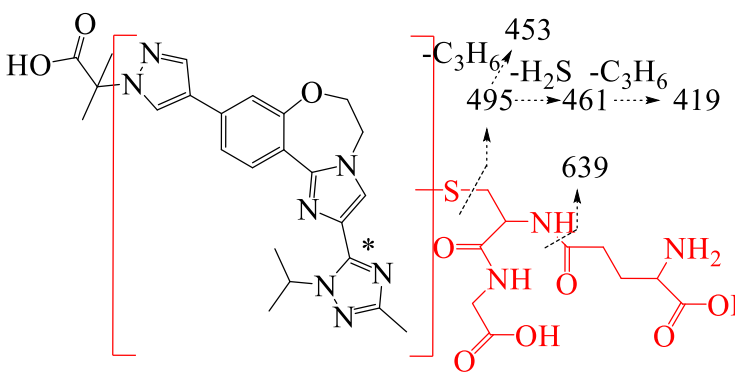
⁵Current affiliation: Clinical Pharmacology, Seagen, South San Francisco, CA

Corresponding author:

Laurent Salphati, Pharm.D., Ph.D.

Drug Metabolism and Pharmacokinetics, Genentech, Inc., 1 DNA Way, South San Francisco, CA
94080. Phone: 650-467-1796. Email: salphati.laurent@gene.com

Supplementary Table S1. Summary of structures and mass fragmentation for metabolites of Taselisib in rats, dogs and humans.

Analyte	Observed MH ⁺ (Chemical formula)	Source	Structure
Taselisib	461.2408 (C ₂₄ H ₂₉ N ₈ O ₂ ⁺)	Rat: P, U, F, B Dog: P, U, F, B Human: P, U, F	
M1 (Oxidation to carboxylic acid)	*493.2182 (¹⁴ CC ₂₃ H ₂₇ N ₈ O ₄ ⁺)	Rat: B	 <p>or</p> <p>[M+H]⁺=493 491-H₂O= 473 493-CO₂=449 449-NH₃=432 449-C₃H₆=407 432-CO=404 449-NH₃-C₃H₆=39</p>
M2 (Glutathione conjugation)	*768.3123 (¹⁴ CC ₃₃ H ₄₄ N ₁₁ O ₈ S ⁺)	Rat: B	

Supplementary Table S1 (continued). Summary of structures and mass fragmentation for metabolites of Taselisib in rats, dogs and humans.

Analyte	Observed MH ⁺ (Chemical formula)	Source	Structure
M3 (oxidation)	*479.2389 (¹⁴ CC ₂₃ H ₂₉ N ₈ O ₃ ⁺)	Rat: B	
M4 (oxidation & glucuronidation)	*655.2713 (¹⁴ CC ₂₉ H ₃₇ N ₈ O ₉ ⁺)	Rat: B	
M5 (Di-oxidation)	493.2306 (C ₂₄ H ₂₉ N ₈ O ₄ ⁺)	Rat: F, B Human: F	
M6 (Oxidative ring opening)	493.2306 (C ₂₄ H ₂₉ N ₈ O ₄ ⁺)	Rat: B Human: F	

Supplementary Table S1. Summary of structures and mass fragmentation for metabolites of Taselisib in rats, dogs and humans.

Analyte	Observed MH ⁺ (Chemical formula)	Source	Structure
M7 (Oxidation & sulfation)	*559.1958 (¹⁴ CC ₂₃ H ₂₉ N ₈ O ₆ S ⁺)	Rat: B	
M8 (Oxidation)	*479.2390 (¹⁴ CC ₂₃ H ₂₉ N ₈ O ₃ ⁺)	Rat: U	
M9 (Amide hydrolysis)	*462.2248 (C ₂₄ H ₂₈ N ₇ O ₃ ⁺)	Rat: F, B Dog: P, U, F, B Human: U, F	
M10 (Oxidation)	477.2370 (C ₂₄ H ₂₉ N ₈ O ₃ ⁺)	Rat: P, U, F, B Dog: P, U, F, B Human: U, F	

Supplementary Table S1 (continued). Summary of structures and mass fragmentation for metabolites of Taselisib in rats, dogs and humans.

Analyte	Observed MH ⁺ (Chemical formula)	Source	Structure
M11 (Oxidation)	477.2359 (C ₂₄ H ₂₉ N ₈ O ₃ ⁺)	Rat: U, F, B Dog: P, U, F, B Human: U, F	
M12 (Acetylation & ring opening)	*479.2392 (¹⁴ CC ₂₃ H ₂₉ N ₈ O ₃ ⁺)	Rat: B	
M13 (Oxidation & glucuronidation)	*655.2710 (¹⁴ CC ₂₉ H ₃₇ N ₈ O ₉ ⁺)	Rat: U, F, B	
M14 (Methylation & Oxidation)	491.2526 (C ₂₅ H ₃₁ N ₈ O ₃ ⁺)	Dog: P, U, F, B	

Supplementary Table S1 (continued). Summary of structures and mass fragmentation for metabolites of Taselisib in rats, dogs and humans.

Analyte	Observed MH ⁺ (Chemical formula)	Source	Structure
M15 (Methylation & hydrolysis)	476.2416 (C ₂₅ H ₃₀ N ₇ O ₃ ⁺)	Dog: P, U, F, B	
M16 (Methylation & oxidation)	491.2525 (C ₂₅ H ₃₁ N ₈ O ₃ ⁺)	Dog: P, U, F, B	
M17 (Methylation)	475.2571 (C ₂₅ H ₃₁ N ₈ O ₂ ⁺)	Dog: P, U, F, B	

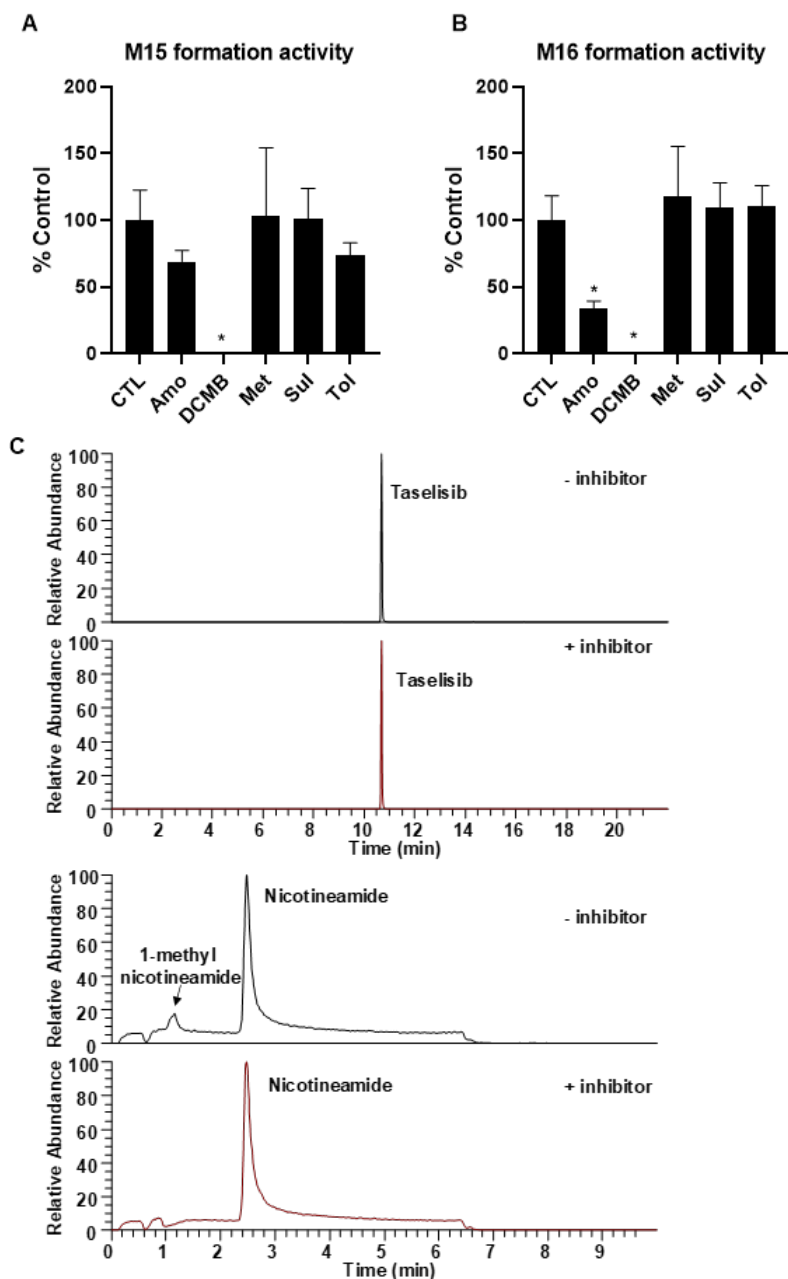
*; m/z values of an analyte and its fragments were based on [¹⁴C] compounds.

Supplementary Table S2. ^1H and ^{13}C NMR Data for GDC-0032 and M17 (δ in ppm)

Position	GDC-0032 ^a		M17 ^a	
	^{13}C	^1H , multiplicity (<i>J</i> in Hz)	^{13}C	^1H , multiplicity (<i>J</i> in Hz)
1	131.8	8.41, d (8.4)	131.8	8.43, d (8.4)
2	121.0	7.37, dd (1.8,8.4)	120.8	7.41, dd (1.8,8.4)
3	117.3	---	116.2	---
4	118.1	7.30, d (1.8)	118.0	7.36, d (1.8)
5	158.0	---	158.3	---
6	136.4	---	137.1	---
7	146.8	---	148.8	---
9	131.3	---	122.2	---
10	124.8	7.71, s	128.9	8.19, s
12	51.5	4.52, m	51.7	4.64, m
13	70.0	4.52, m	69.5	4.59, m
14	123.2	---	122.8	---
15	138.8	7.97, brs	138.6	7.99, brs
18	127.5	8.27, d (0.5)	127.3	8.29, d (0.5)
19	66.6	---	66.2	---
20	177.9	---	177.7	---
21	26.4	1.86, s	26.0	1.87, s
22	26.4	1.86, s	26.0	1.87, s
23	149.5	---	146.4	---
26	160.3	---	154.7	---
28	52.4	5.91, sep (6.6)	55.4	5.52, sep (6.6)
29	22.7	1.54, d (6.6)	21.8	1.62, d (6.6)
30	22.7	1.54, d (6.6)	21.8	1.62, d (6.6)
31	13.7	2.36, s	10.6	2.64, s
32			33.6	3.95, s

^a. Measured in methanol-*d*₄ with ^1H at 500 MHz, and ^{13}C at 125 MHz. The ^{13}C NMR signals for M17 were indirect from HSQC and/or HMBC spectra.

d: doublet; dd: double doublet; s: singlet; brs: broad singlet; sep: septet; m: multiplet.



Supplementary Figure S1. Characterization of methyltransferase involved in inavolisib

metabolism in dogs. (A & B) Taselisib was incubated with dog hepatocytes in the presence of various human methyltransferase inhibitors for 3 h: Amo; amodiaquine (HNMT inhibitor), DCMB; 2,3-dichloromethylbenzylamine (TMT inhibitor), Met; 1-methyl nicotinamide (NNMT inhibitor), Sul; sulfasalazine (TPMT inhibitor), Tol; tolcapone (COMT inhibitor). (C) Recombinant NNMT was incubated with taselisib or nicotine amide for 1 hours in the presence of 5-amino-1-methylquinolin-1-ium iodide (NNMT inhibitor). *: $p < 0.05$ compared to CTL from student t-test.